PHYSICAL REVIEW B VOLUME 27, NUMBER 4 15 FEBRUARY 1982

Electronic structure of Ni and Pd alloys. I. X-ray photoelectron spectroscopy of the valence bands

John C. Fuggle, F. Ulrich Hillebrecht, R. Zeller, Zygmunt Zołnierek,* and Peter A. Bennett†
Institut für Festkörperforschung, der KFA Jülich, D-5170 Jülich, Federal Republic of Germany

Ch. Freiburg
Zentralinstitut für Chemische Analyse IV, der KFA Jülich, D-5170 Jülich, Federal Republic of Germany
(Received 11 May 1982)

X-ray photoelectron (XPS) spectra of the valence bands of approximately 60 Ni and Pd alloys and intermetallic compounds with 20 different elements are presented. In alloys with electropositive elements the Ni and Pd *d*-band centroids move to larger binding energies and the density of *d* states at the Fermi level (E_F) is greatly decreased, indicating that the Ni and Pd *d* bands are being filled. The Ni and Pd *d* bands become narrower in alloys with electropositive elements. It is shown that in such alloys, the Ni-*M* or Pd-*M* interactions give a significant contribution to the Ni and Pd bandwidths. This contribution is larger when the second element *M* has a large density of states at the energy of the Ni or Pd *d* bands in the alloy. As this contribution is small in systems that form complicated structural types and glasses we speculate that its absence helps stabilize such structures. The satellite at ~ 6 eV in the XPS spectrum of Ni is found to weaken and shifts to higher binding energy in alloys with electropositive metals. In the twelve alloys where its intensity is large enough to allow us to identify its energy, the binding energy of the satellite agrees with the two-electron binding energy of the Ni ^1G d^8 term derived from Auger spectroscopy. The site- and symmetry-selected densities-of-states curves were calculated for 14 of the alloys to show that this filling is largely due to changes in the hybridization of the Ni or Pd *d* bands with the partner element bands. The actual transfer of Ni and Pd *d* electrons is probably small. These observations are used to rationalize published results of specific-heat and magnetic measurements on such alloys.

I. INTRODUCTION

The main purpose of this paper is to report on trends in the electronic structure of Ni and Pd alloys and intermetallic compounds with about 20 other metallic elements spread across the whole Periodic Table. Several factors led to the choice of Ni and Pd alloys for this study. Firstly, the Ni and Pd *d* states have large photoelectron cross sections, so that it is usually possible to pick out the peaks due to such states in the valence-band (VB) spectra. Secondly, it was also known that Ni, and to a lesser extent Pd, show interesting many-body effects in their valence-band and core-level spectra[1–18] as well as their *XVV* Auger spectra[19–26] so that a combination study was attractive. Thirdly, some preliminary studies[27] indicated that the valence core-level spectra were strongly sensitive to the chemical environment in alloys. Lastly, Ni forms a great variety of intermetallic compounds and alloys so that a systematic study across the whole Periodic Table is possible.

Parts II and III of this series [subsequently referred to as paper II (Ref. 28) and paper III (Ref. 29)] deal with information from x-ray photoelectron spectroscopy (XPS) of the core levels, and Ni L_3VV Auger spectra, respectively. This paper is a report on valence-band properties as studied by XPS and theoretical calculations. The XPS spectra yield information on the excited states of the alloys, while the calculations yield the density of states for the *ground* state.

Many of the numerous photoelectron studies of Ni and Pd started from the ground-state properties of Ni or Pd and explored the role of many-body effects in the photoelectron spectrum.[1–18] The many-body effects lead to satellites in the XPS spectra, and small shifts between peaks in the XPS spectra and the calculated densities of states. Although we do collect together data on the satellites

(Sec. V A) and the discrepancies between theory and experiment (Sec. V E) our main aim is different. We start from the photoelectron spectra, and, knowing some of the effects of many-body interactions, we seek information on the ground states. We use the XPS spectra as a measure of the position and widths of the Ni and Pd bands and the calculations to help with peak assignments. The calculations also give us our main source of information on mixing of the different orbitals in the alloys and occupation numbers for the Ni and Pd *d* states. In paper II we will show that the results from core-level XPS support our deductions on charge transfer and mixing of the orbitals.

In order to formulate and test statements on the trends in electronic structure it was necessary to collect data on many alloys. XPS spectra of ~ 60 alloys and 14 calculated densities of states are presented in Sec. IV and are correlated with previous data on the same systems (e.g., electronic specific heats for Al-Ni alloys or saturation magnetic moments). Section IV is necessary for the specialist in various alloy systems, but for the general reader the discussion section of this paper is more important. It is in the discussion that the trends in bandwidths and positions are examined. It is shown there that XPS spectra from Ni and Pd alloys, as well as a large amount of literature data on electronic specific heats and magnetic properties, can be related to a simple picture of electronic structure. We will also incorporate into the discussion many results from PS studies of small groups of alloys that have been reported (see, e.g., Refs. 30–41).

Another parameter in the electronic structure, besides bandwidths and positions, which is of special interest for theories of alloy stability is the degree of charge transfer between the atoms. This has been a subject of many discussions in deliberations about alloy stability over the last 40 years (see, e.g., Refs. 42–45) and not just during the renewed interest in semiempirical schemes over the last four years.[36–58] The very successful scheme of Miedema for predicting the signs, and even sizes of heats of formation,[47–49] was originally tied to the concept of charge transfer. On the basis of their chemical potential model, Alfonso and Girifalco concluded that charge transfer was present and important in alloys.[50] However, Williams *et al.*[52] concluded that charge transfer was unimportant in alloys between transition metals where they believed bonding was due to "pervasive changes in the valence band driven by nondegeneracy of the constituent *d* levels." On the basis of calculations[51–57] and comparison with Knight shifts in nuclear-magnetic-resonance and Mössbauer shifts[53–58] the concensus of opinion seems to be moving towards the idea that charge transfer in the *d* electrons is small. Watson *et al.*[53–57] have concluded that the *d*-electron transfer in alloys involving transition or noble metals is small and may be actually in the opposite direction to that expected on the basis of electronegativity considerations. Such transfer would then be overcompensated by *s*- and *p*-electron transfer.[53–58] On the other hand, models used to explain the chemical and physical properties of Ni and Pd alloys have often used the idea that the Ni or Pd *d* bands are filled in alloys with electropositive metals. The picture we use to describe data on alloys with electropositive metals, is one where the Ni or Pd *d* bands become filled by hybridization rather than transfer of charge to the *d* orbitals on the Ni or Pd site.

II. CALCULATIONS AND HYBRIDIZATION, CORRELATION, AND CROSS-SECTION EFFECTS

It is conventional to believe that band structures are not strongly dependent on crystal structure. This means that small changes in structure do not produce large changes in bandwidths or their centroid positions or in the mixing of bands but may cause changes in the structure within the band. We believe this may not be true for highly compact structures, such as Laves phases, where the interatomic distances can be very small, and do not attempt calculations relating to these structures here. For this work the densities of states were calculated for 14 intermetallic compounds with 1:1 or 1:3 stoichiometry. Some of these have structures distorted from cubic at room temperature (see Tables VII and VIII) for which we have no computational schemes. In these cases we made calculations for the compounds in CsCl or Cu_3Au structures with the same density as found in nature. The calculations were performed with the band-structure method of augmented spherical waves.[59] Density-functional theory in the local-density approximation was applied to self-consistently determine the electronic potential. For the exchange-correlation part of the potential the Hedin-Lundqvist form[60] was used. In order to facilitate the comparison with the experiments we applied Gaussian broadening to the calculated densities of states. The width of this broadening was chosen as 0.6 eV, which is the reso-

lution function of the instrument as used here. This broadening thus includes no damping due, for instance, to lifetime broadening.

It is constructive to consider here the electronic structure of Ni and the results of the calculations for one alloy to help put our investigations in context. It is generally agreed that the d band of Ni contains about 9.4 electrons on the basis of the saturation magnetic moment.[61,62] However, a population analysis of the linear combination of atomic orbitals wave functions indicates that the number of d electrons is only of the order of 8.8.[63] These results indicate that there must be some d character in the unoccupied sp states of Ni and we assume that there can be some in the Ni (or Pd) alloys studied here.

In Fig. 1 we present the calculated density of states for ScNi. The Sc d and Ni d states have been projected out of the total density of states (DOS) and are also shown. The Ni d character is concentrated in states below E_F while the Sc d is concentrated above E_F. However, there is some Ni d character indicated in the unoccupied states. Analysis of the nature and quantity of this unoccupied d character by theoretical methods can, in principle, give information on the charge transfer to or from the Ni d states. Difficulties arise because of ambiguity in defining the boundaries of the Ni atoms, but the calculations generally indicate small changes in the numbers of d electrons—of the order of 0.3 electrons in alloys.[53–57,64]

Exact analysis of the nature of the unoccupied d character also presents special difficulties. In particular both high-energy plane waves and the tails of wave functions centered on the neighboring atoms can be expanded in terms of wave functions centered on the Ni site so that some of these have d character.[65] The d character arising from both plane waves and the tails from other atoms has a radial distribution which is very different from that from true Ni d orbitals, but a theoretical analysis of the radial functions is not trivial. The effects of both plane waves and the tails are more important at high energies. The calculated density of states of ScNi in Fig. 1 supports our contention that neither effect is very important in the 5-eV interval above E_F. Notice that the Ni d character goes to zero about 5 eV above E_F. Now the role of the plane waves increases with energy, so that if their contribution is zero at 5 eV above E_F, it will also be zero at lower energies which means we can neglect their contribution in Fig. 1, and by implication, in the other alloys studied here. Notice also that in the region above E_F the Ni d state density shows peaks at the same energies as the Sc d-state peaks. This could, at first sight, be taken as evidence of spillover of charge from Sc sites. Nevertheless we argue that this is not the case because the Ni d-state density is not directly proportional to the density of Sc states, but tails off at higher energies where we intuitively expect the Sc d wave functions to be more distended. Also the Sc d character in the occupied bands peaks at slightly lower energies than the Ni d-state density. These characteristics are suggestive of mixing of Ni d and Sc d character. This mixing or redistribution will prove very important in interpretation and discussion of our experimental results. The idea that the Ni d bands can become completed, or filled, without excessive charge transfer due to mixing will be seen to explain the photoemission results and also the role of some electron-atom ratios in alloy stability and chemical trends.

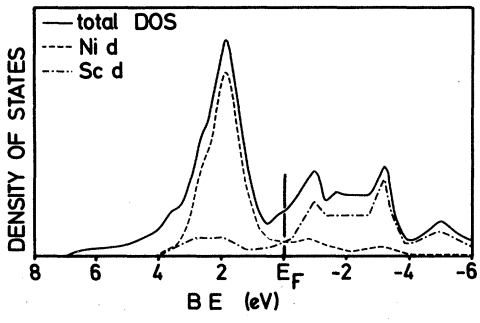

FIG. 1. Computed DOS curves for ScNi showing the partial densities of Ni and Sc d character.

Two major effects lead to differences between measured XPS valence bands and the one-particle densities of states: cross-section effects and correlation effects. The most widely used partial photoionization cross sections for the valence-band electrons are those given by Scofield's atomic calculations.[66] In Table I we have converted Scofield's values for Al $K\alpha$ radiation to cross sections per electron relative to his value for Ni $3d$ electrons. The values are tabulated for all the elements considered in this study, and it will be recognized that for almost all the alloys studied, the cross sections for electrons in Ni and Pd d orbitals are considerably higher than those of the partner element. In addition the number of Ni or Pd d electrons per atom is usually higher than the number of valence electrons from the partner element, so that the Ni and Pd d states usually dominate the valence-band spectra. The major exceptions are alloys with noble

TABLE I. Calculated cross sections per valence electron [these values are calculated using the partial cross sections of Scofield (Ref. 66) and the configurations for the gas-phase atoms] at 1487 eV, σ relative to Ni $3d$ for the elements studied.

Element	VB electron	σ
Mg	$3s$	0.29
Al	$3s$	0.54
Al	$3p$	0.07
Sc	$3d$	0.08
Ti	$3d$	0.14
V	$3d$	0.21
Cr	$3d$	0.33
Ni	$3d$	1.00
Ni	$4s$	0.56
Cu	$3d$	1.18
Y	$4d$	0.62
Nb	$4d$	0.99
Pd	$4d$	2.48
In	$5p$	0.39
La	$5d$	1.00
Ce	$6s$	0.22
Ce	$4f$	1.40
Ta	$5d$	1.86
Au	$5d$	3.63
Th	$7s$	0.22
Th	$6d$	0.95

metals where the noble-metal d electrons have a higher cross section and an unambiguous identification of the Ni $3d$ or Pd $4d$ electron contribution to the spectra is less easy.

The second class of differences between the calculated DOS and the XPS valence-band spectra are due to exchange-correlation effects. In this work the DOS is calculated within the density-functional formalism of Hohenberg, Kohn, and Sham.[59,60,67–69] Although the eigenvalues produced in this formalism have no strict physical meaning they usually give a reasonable estimate of excitation energies as measured by photoemission. Discrepancies between experimental and density-functional values do arise, however, because calculation of the true excitation spectrum requires introduction of nonlocal self-energy effects in the exchange-correlation term.[67] Unfortunately, this is difficult, even when approximations are made (see, e.g., Refs. 12–15 and 69–71) and cannot be attempted here. Two forms of discrepancy between experimental photoemission spectra and eigenvalue densities calculated in the local-density-functional formalism are known. The first is that the local formalism eigenvalues for localized levels are shallower than found by experiment and the discrepancy increases with increasing localization; for instance in Cu,[69,72,73] Zn, and Gd.[74–76] The $3d$ positions are, respectively, $\sim$0.3, $\sim$1.0, and $\sim$2.3 eV shallower than in experiments.

The second form of discrepancy arises in unfilled bands in the presence of correlation effects. Its importance increases with the size of intra-atomic correlation between the valence electrons and so is more important for Ni (Refs. 1–17) than Fe (Refs. 77 and 78) or Pd.[8] It leads to satellite structure in photoelectron spectra of the Ni $3d$ or Pd $4d$ states.[1–18] The basic physics behind the processes can be explained using Fig. 2. In this simplified picture the Ni or Pd wave function is written in terms of atom like d^9 and d^{10} configurations. The final states, after VB photoionization, correspond quite closely to d^8 and d^9 configurations and arise from the two terms in the ground state. The intra-atomic Coulomb interaction between holes localized at a single Ni or Pd site is several volts and causes the d^8 term to have larger energy than the d^9 terms. The d^8 contribution to the spectrum thus appears as a satellite at higher binding energy (BE) in the photoelectron spectrum. The so-called d^8 final-state configuration is degenerate with band states. States at the bottom of the d bands give a larger contribution to the satellite than states at the top of the band so that the observed band is distorted with respect to the calculated density of states.[1–18]

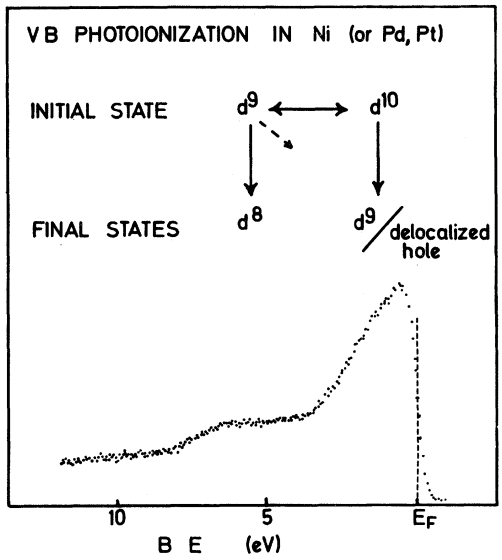

FIG. 2. Schematic diagram of the interpretation of VB emission from Ni and Pd alloys, illustrated with the case of Ni.

We warn the reader than the above description is an oversimplification and does not contain all the physics of the situation (see Refs. 12–16). In particular it should be recognized that the relative weight of the satellite and bandlike parts of the spectrum are not equal to the relative weights of the "d^9" and "d^{10}" contributions to the ground-state wave function as indicated in a very schematic way by the diagonal arrow in Fig. 2. However, for a given bandwidth the trends in relative satellite intensity will be expected to decrease as the Ni 3*d* or Pd 4*d* bands are filled. A second complication is that if hybridization is taken into account the descriptions d^9 and d^{10} are inaccurate because the *d* states always contain some "*s*" character. By d^9 configuration we really mean configurations with one unpaired hole in *d*-like states.

III. EXPERIMENTAL

Information on the stoichiometry of the alloys and intermetallics which can be prepared is contained, for the most part, in Refs. 79–82. These references and Refs. 83–86 served as sources for the structural information on the materials used and to save space we only refer to the primary literature in special cases.

The alloys and intermetallic compounds studied here were mostly prepared by melting the constituents together under ~700-mm clean argon with rf heating in a water-cooled copper hearth (cold-crucible method). The only exceptions to this procedure were the magnesium alloys which were prepared under high argon pressures (100 bar) to reduce loss of magnesium by evaporation. Samples were examined metallographically after melting and when necessary annealed in a vacuum of 10^{-8} Torr to reduce the amount of secondary phases or eutectics present, as determined metallographically. A final check on the materials was made using x-ray powder diffractometry. Many of the samples studied do not melt congruently, but form via peritectic reactions in the solid state between a more stable phase and eutectic regions. In our experience, it was only possible to form single-phase alloys of many of these peritectic compounds in small pellets. However, for all of our sample purity checks and measurements we required 1 cm^3 of material, which is quite a large pellet in these terms. Thus in some cases the samples contained small amounts ($<5\%$) of secondary phases. These do not significantly affect the XPS spectra and these samples are preferable to small uncharacterized pellets. There was one sample (TaNi) which gave particular problems and which always contained ~20% of secondary phases. As TaNi is reported to have the W_6Fe_7 structure[87] and x-ray diffraction did show the presence of material with this structure, we attempted to prepare Ta_6Ni_7 in case the stoichiometry of the compound had been wrongly stated in the literature. This did not help and we were forced to use a TaNi sample with ~20% of a second phase, which probably causes some broadening of the spectral features.

In the course of these investigations we prepared some compounds that were not previously known, or whose structures are unknown. Characterization of these relied more heavily on the metallographic data as the x-ray-diffraction patterns could not be indexed and were only useful as a check for the presence of other, known binary phases.

The published La-Ni phase diagram[88,89] shows only one La-rich intermetallic compound with the stoichiometry La_3Ni. We examined samples with the stoichiometries La_7Ni_3 and La_3Ni. La_3Ni was annealed for three days at 480 °C and 1 day at 430 and 380 °C. Both samples had only 2% second phase as indicated by metallography. La_7Ni_3 had the Th_7Te_3 structure found by Fisher *et al.*[90] The diffractogram of La_3Ni was not similar to that of La_7Ni_3 and showed no La lines. We conclude that both La_3Ni and La_7Ni_3 exist as discrete single phases.

CePdAl and LaPdAl have not been reported, but the analogous Th compound is known.[91] The compounds formed directly from the melt. They were extremely brittle so that small pieces broke away from the surface during polishing for metallography, but apart from ambiguities arising from this source the LaPdAl and CePdAl samples were nearly single phase with 1–2 % segregation of a second phase in the grain boundaries and in the grains of La- or Ce-PdAl. The ThPdAl sample had approximately 7% of a second phase. In metallographic analysis of the samples with polarized light the reflectivity of the individual grains was very different, indicating optical activity and a complex crystal structure. The x-ray diffractograms were complex and we could not determine the crystal structure type although we did not find any of the known binary phases to be present. We conclude that compounds LaPdAl and CePdAl do exist.

The spectra were measured in a ultravacuum instrument incorporating analyzer and electronics from a Kratos ES 300 spectrometer. The spectra

were for the most part excited with Al $K\alpha$ radiation from a specially constructed, large solid-angle monochromator with 54 quartz single crystals on a toroidal substrate.[92] The total instrumental resolution used for these studies was 600-meV full width at half maximum (FWHM) and studies of the Fermi-level cutoff showed the instrument function to be Gaussian, within experimental error.

The samples were cleaned *in situ* by scraping with an aluminum oxide file. In some cases the mechanical working of the sample caused a pressure rise to $3-4\times10^{-10}$ Torr, but pressures of 1×10^{-10} Torr were more typical. Typical base pressures in the measurement chamber were 5×10^{-11} Torr. By scraping at intervals of less than 8 h it was possible to make all measurements on sample surfaces contaminated with less than approximately 3 at. % of oxygen and carbon (combined). The level of contamination was estimated from the intensity of the O 1*s* and C 1*s* XPS peaks relative to the metal peaks and Scofield's calculated photoemission cross section.[66] Surface segregation could be a severe problem in measurements on alloys, and has been proven in the case of alloys cleaned by sputtering and heating. In some cases we used Scofield's calculations[66] and the measured XPS peaks intensities from scraped samples to make a semiquantitative analysis of the surface layer and found no significant evidence for surface segregation, with the possible exception of CuNi.

IV. RESULTS AND INTERPRETATION

A. Ni alloys with Mg and Al

These alloys are treated together because Mg and Al are both usually considered as simple metals and both form well-defined intermetallic compounds with Ni. The XPS spectra of the compounds are shown in Figs. 3 and 4 and band positions and widths are given in Table II. The spectra are dominated by the peaks from the Ni *d* bands, which are observed to move away from E_F as Mg or Al is added. The *d*-band peaks also become narrower and more symmetric and the satellite shoulder at 6 eV, attributed to d^8-like final states, becomes noticeably weaker and shifted to higher binding energy as the Ni concentration decreases. At high Al or Mg concentration, surface-plasmon losses may also play a role in the satellite region (see paper II). The spectrum of AlNi shown here is in reasonable agreement with previously published XPS data.[35,41]

The total density of states at E_F can be roughly estimated from specific-heat measurements although corrections for electron-electron and electron-phonon mass enhancement should really be taken into account for accurate estimates.[93] The experimental totals in states eV^{-1} $atom^{-1}$ (Ref. 94) are Ni=2.97,[95] $AlNi_3$=2.75,[96] AlNi=0.55,[97]

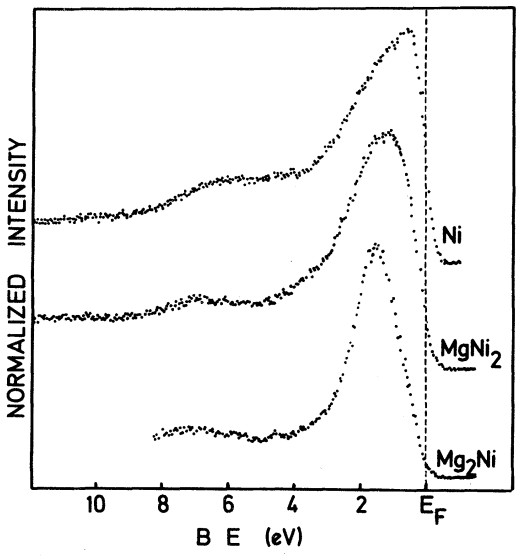

FIG. 3. XPS VB's from Ni, $MgNi_2$, and Mg_2Ni.

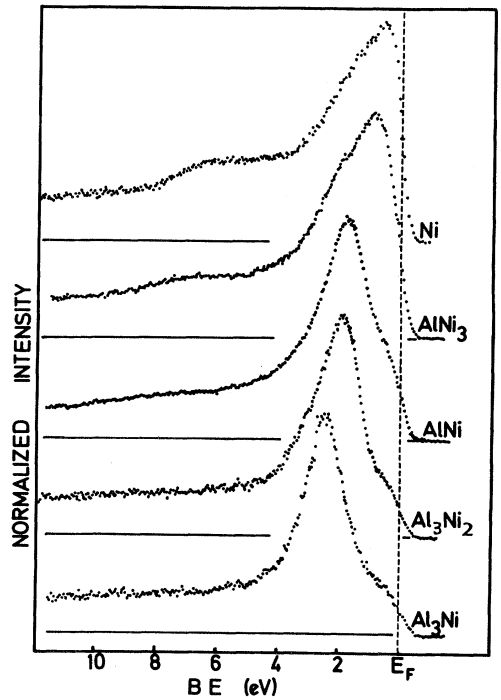

FIG. 4. XPS VB's from Ni, $AlNi_3$, AlNi, Al_3Ni_2, and Al_3Ni.

TABLE II. d-band properties in Ni alloys (all values in eV).

Material	Peak BE	±	Centroid BE	W^a	FWHM	Satellite BE	±
Ni	0.60	0.1	1.4	4.3	2.4	6.1	0.5
$MgNi_2$	1.10	0.2	1.4	3.3	1.6	6.7	0.5
Mg_2Ni	1.30	0.2	1.35	2.75	2.3	6.7	0.5
$AlNi_3$	0.90	0.3	1.50	4.0	2.5	6.7	0.5
AlNi	1.75	0.3	1.85	3.5	2.3	7.7	0.5
Al_3Ni_2	1.90	0.2	2.15	2.85	1.7		
Al_3Ni	2.50	0.2	2.5	2.4	1.5		
ScNi	1.45	0.2	1.6	3.25	2.1	7.1	0.5
TiNi	1.70	0.2	1.75	3.8	2.4	7.2	0.5
$CrNi_2$	1.10	0.2	1.6	4.05	2.6	6.8	0.5
CuNi	0.75	0.2	obscured by Cu d bands				
PdNi			obscured by Pd d bands				
InNi	1.15	0.2	1.35	3.05	2.0	6.6	0.5
$TaNi_3$	0.9	0.2	1.4	4.25	2.8	6.5	0.5
$TaNi_2$	1.7	0.2	2.0	4.15	2.9	7.7	0.5
Ta_2Ni	1.85	0.3	2.1	4.2	3.0		
AuNi	0.7	0.2	1.1	obscured by Au d bands			

[a]Determined as described in Appendix.

$Al_3Ni=0.53$,[98] $Al=0.58$.[93] These values are in good agreement with the experimental XPS data where we see no large drop in the ratio of the intensity at E_F to the intensity in the peak from Ni to $AlNi_3$, but much smaller ratios in AlNi and Al_3Ni. This is difficult to illustrate clearly in Fig. 4, but in Ni and $AlNi_3$ the Fermi level, as defined by parallel studies of Au or Pd, was within 50 MeV of the half-height of the peak. In AlNi, Al_3Ni_2, and Al_3Ni the Fermi level is situated on the edge of shoulders on the low-BE side of the main peaks.

Comparison of the observed XPS spectra with the results of density-of-states calculations is useful here and we chose the Al-Ni systems for this because these are structurally simpler. Calculations for AlNi could be made in the observed CsCl structure. Al_3Ni has the complicated DO_{20} orthorhombic structure, which is not suitable for computation so the calculations were made for Al_3Ni in the Cu_3Au structure with the same density as Al_3Ni. The calculated results for all three alloys computed are in agreement with those of Hackenbracht and Kübler,[64] but have been broadened with a 0.6-eV Gaussian function to allow for the instrumental resolution.

Starting with Al_3Ni in the lower panel of Fig. 5, we find the peak in the XPS spectrum to be well reproduced by the calculated density of Ni d states, although the calculation places the peak ~ 0.6 eV nearer to E_F. The calculation also gives additional structure which might change if we could make the calculation in the DO_{20} structure. The intensity at lower kinetic energy (higher BE) due to inelastically scattered electrons masks any intensity due to photoemission from the Al sp bands. The shoulder in the XPS spectrum at E_F is attributed to states with mostly Al character, in agreement with the calculations which suggest only 20–30% Ni d character in this region.

The comparison of experimental and theoretical results for AlNi yields less satisfactory results. In XPS the calculated Ni d bands are clearly at higher binding energy than in experiment. In addition the d-band shape is poorly reproduced; the calculation indicates a skewing of the peak to higher BE that is not present in the experiment when we allow for the effects of inelastic scattering and the "d^8-like satellite."

Information on the site- and symmetry-selected density of states is also available from x-ray photoelectron spectra.[99] Because x-ray-emission matrix elements are so highly localized the Al x-ray spectra from Al-Ni alloys is strongly related to the density of Al states. Also dipole selection rules cause the Al $L_{2,3}$ ($2p \leftarrow V$) emission to be dominated by the Al s and d states, whereby the contribution of the Al d states is low because their occupation is low. The Al d states may be totally neglected at BE's greater than 4 eV. The middle section of Fig. 5 compares the Al $L_{2,3}$ x-ray-spectrum AlNi with the calculated density of Al s states. There is an overlap of the Al $L_{2,3}$ spectrum with the Ni $M_{2,3}$ ($3p \leftarrow 3d$) emis-

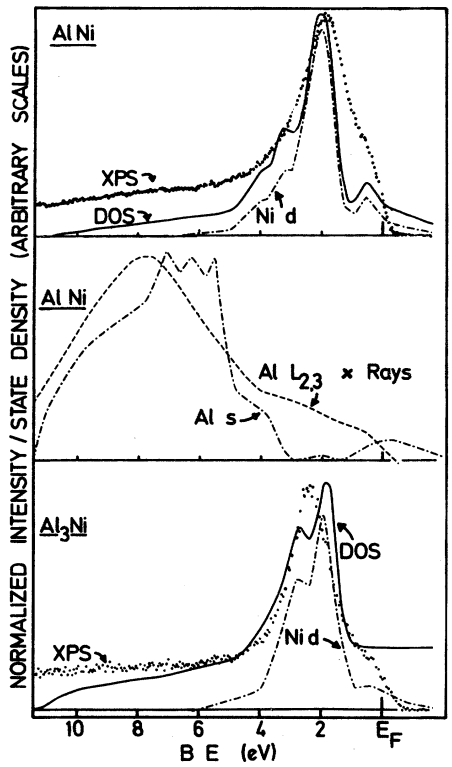

FIG. 5. Top: Comparison of the observed AlNi XPS VB spectrum with the calculated total DOS, broadened by a 0.6-eV Gaussian function. The two curves have been normalized at the peak maxima. Also shown is the broadened, calculated density of Ni *d* states, to the same scale as the full DOS curve. Middle: Comparison of the AlNi $L_{2,3}$ x-ray-emission spectrum from Ref. 121 with the calculated, unbroadened density of Al *s* states. Curves have been normalized at the peak maxima. Lower: Comparison of the observed XPS spectra and calculated total Al_3Ni DOS. Other details as in upper part of figure.

sion which is in a peak at 8-eV BE and contributes approximately 15% to the total-emission spectrum. Despite the interference of the Ni $M_{2,3}$ emission the discrepancies between calculation and experiment are significant and warrant further consideration. The absence of the three-peak structure in the x-ray spectrum, calculated to occur at 5—7 eV, may be related to lifetime-broadening effects, which are not included in the calculation. Lifetime-broadening effects can be large. However, we believe there is a real discrepancy in the centroids of the main Al-state band as calculated, and the main Al $L_{2,3}$ emission peak in AlNi that is too large to be explained by matrix-element variation through the band (see e.g., Refs. 100 and 101). We shall return to this point in Sec. IV E of the discussion, after presentation of Al-Pd results, where there is no interference of Al and Pd x-ray emission, as discussed in Sec. IV E.

B. Ni alloys with Sc, Ti, Cr, In, and Ta

Sc, Ti, and Ta were chosen as fairly typical examples of the early transition metals. In alloys of Sc and Ti with Ni the Ni *d* bands still dominate the XPS spectra, which is not the case for the transition metals to the right of the Periodic Table as illustrated in Table I and later sections. The cross sections for the metal *d* electrons also increases from the first to the second to the third rows of transition metals. Cr is an example of a transition metal in the middle of the series. Ni forms stable, 1:1, intermetallic compounds with early transition metals, but not with elements in the middle of the transition metals series so we chose to study $CrNi_2$ which forms from solid solutions at 550 °C. It was chosen as an example of the *B* group elements.

The XPS spectra in Fig. 6 show that the density of Ni *d* states at the Fermi level has dropped with

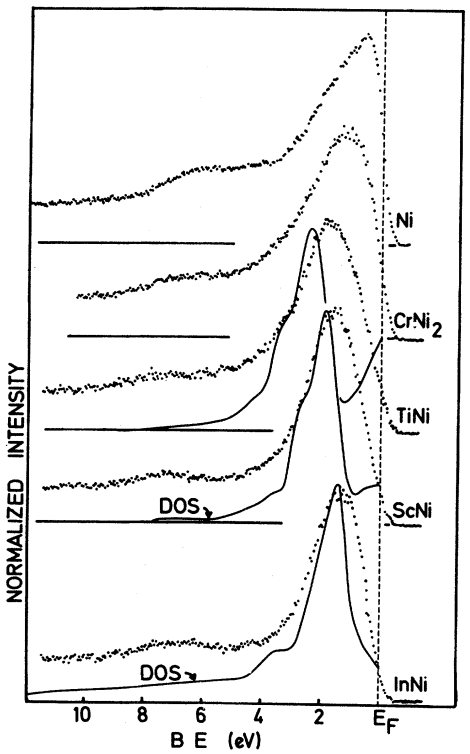

FIG. 6. XPS VB spectra from Ni, $CrNi_2$, TiNi, ScNi, and InNi. Calculated total DOS curves, broadened by a 0.6-eV Gaussian function, are also given for TiNi, ScNi, and InNi.

respect to Ni in $CrNi_2$, TiNi, ScNi, and InNi. In all cases the intensity in the region of the d^8 satellite also drops, indicating that the influence of the d holes has dropped. The total Ni d bandwidth also drops in the alloys in the order Ni $\sim CrNi_2 > TiNi > ScNi > InNi$ (see Table II). This change in width is unlikely to be entirely due to the changes in direct Ni-Ni overlap: ScNi and TiNi both exist in CsCl structures with similar lattice constants (3.15 and 3.01 Å, respectively) and even InNi, which has a complicated structure at room temperature, has a high-temperature modification with CsCl structure with lattice constant equal to 3.09 Å. A more likely explanation for the changes in widths is the change in state density in the region of the Ni d bands on the neighboring site. If we approximate this state density to the number of valence electrons divided by the bandwidth in the element the order is $Ni \sim Cr > Ti > Sc > In$, which is precisely the order of the Ni d bandwidths. Such correlations are discussed more extensively in Sec. V B. The position of the d-band maxima, or centroids with respect to E_F in the alloys shown in Fig. 6 does not follow any obvious pattern.

The agreement between theoretical DOS curves and the XPS spectra for ScNi and InNi is moderately good. In both cases the bandwidths are underestimated by the calculation, and for ScNi the calculated peak due to the d bands is approximately 0.4 eV deeper in the band. However, in TiNi the calculated Ni d peak in TiNi is approximately 1.0 eV deeper than in experiments. The differences between ScNi and TiNi is surprising in view of the similarity of their crystal structures and electronegativities. The DOS calculated by us is quite similar to that found in an augmented-plane-wave calculation[102] indicating the difference between theory and experiment is independent of the theory used.

Calculations of densities of states in Ta alloys would require relativistic treatment and we thus rely on the experimental data in Fig. 7. Scofield's calculated cross sections[66] for the Ta 5d and Ni 3d electrons are comparable (see Table I) and this is borne out by the comparison of the XPS valence-band spectra of Ta and Ta_2Ni which have been normalized to the Ta 4f level before reproduction. It is seen that the photoemission from Ta bands must contribute more than half of the total valence-band photoemission from Ta_2Ni. Comparison with other Ni alloys suggests that the Ta states must be concentrated near E_F in the alloy and the Ni bands must be deeper, but there is no distinct division as

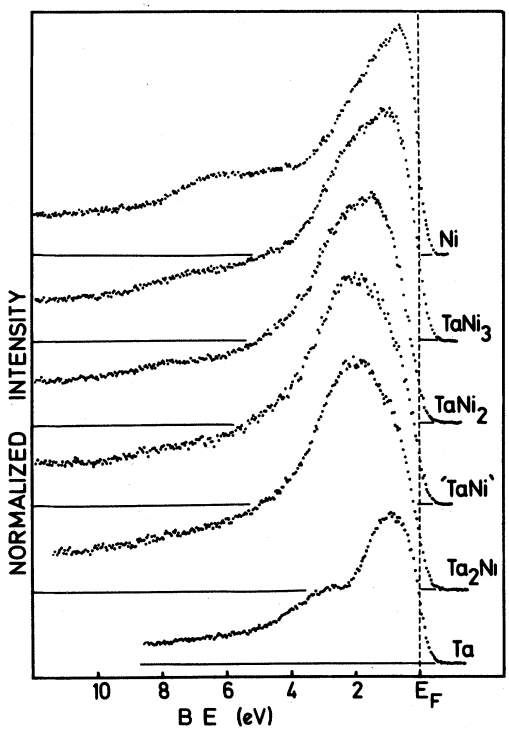

FIG. 7. XPS VB spectra from Ta-Ni alloys. All spectra have been normalized with respect to the maximum VB intensity, except for Ta which was normalized to the Ta_2Ni spectrum using the Ta 4f peak with BE $\sim$ 22 eV.

in other nickel-dilute alloys such as in Al_3Ni (Fig. 4) or La_7Ni_3 (Fig. 9). We can rationalize the spectra in Fig. 7 if we accept that the Ta 5d levels lie above the Ni 3d levels. The centroid of the Ni d bands is at a higher BE in Ta-rich alloys. The DOS at E_F decreases from Ta and Ta_2Ni to TaNi and $TaNi_2$ as the Ta concentration decreases. It then increases again through $TaNi_3$ to Ni as the concentration of Ni 3d states at E_F increases.

The Ni d^8 satellite at $\sim$6 eV decreases with increasing Ta concentration in the Ta-Ni alloys until it becomes lost in the tail of the valence band. As will become clear in the discussion section, this decrease is consistent with the interpretation that the Ni d-state density at E_F drops as the Ni concentration is reduced.

C. Ni alloys with noble metals and Pd

Ni forms solid solutions over the whole composition range with Cu and Pd. With Au, solid solu-

tions can be obtained by quenching, but some clustering into gold-rich and nickel-rich regions is inevitable and we do not claim that the NiAu alloy studied by us has a completely random distribution of the components. Ni and silver are almost completely immiscible, even in the liquid phase. Cu, Pd, and Au belong to the small number of metals whose electronegativity is larger than that of Ni. [The Gordy and Thomas electronegativities are 1.9, 2.0, and 2.3, respectively, as against 1.8 for Ni (Ref. 103)].

Owing to its smaller photoelectron cross section, the contribution of the Ni 3*d* electrons to the XPS spectra of NiCu, NiAu, and NiPd in Fig. 8 is smaller than that of the Cu 3*d*, Au 5*d*, or Pd 4*d*. In addition there may be some surface segregation of Cu in NiCu. However, the peaks near E_F in Fig. 8 can be attributed to states of largely Ni 3*d* character, while the Cu 3*d* and Au 5*d* peaks are found at higher BE, near their positions in the pure elements. In the case of CuNi this picture is in agreement with previous PS investigations and theoretical studies (see, e.g., Refs. 104 and 105).

In NiPd it is not possible to separate *a priori* the contributions of the Ni 3*d* and Pd 4*d* levels to the XPS spectrum. The valence band has a rather square appearance compared with Pd, with enhanced intensity near the bottom of the band (marked with an arrow). However, to associate this extra intensity with states of largely Ni *d* character would imply an unreasonably large shift with respect to Ni metal. In order to resolve this problem we calculated the DOS for NiPd in an *ordered* CsCl structure with the experimental lattice constant for the disordered alloy.[106] We expect the relative positions of the Ni and Pd *d* bands to be reasonably well reproduced by this calculation, although the disorder will smear out any fine structure. The results of the calculation after broadening with a 0.6-eV Gaussian curve are presented in Fig. 8. The total DOS, including Ni and Pd *s* and *p* states, is indicated by the continuous line and has more structure than the experimental curve. This can be at least partially explained by lifetime-broadening effects. The calculated total DOS has generally lower intensity towards the bottom of the band in the region of (2−6)-eV BE, in contrast to the experimental spectrum which is, as mentioned above, rather square. The reason for this becomes clear when we consider the partial densities of Ni *d* and Pd *d* states shown in Fig. 8. The Pd states are more concentrated towards the bottom of the band while the Ni states are near the top. As discussed in connection with Table I the Pd *d* cross section is much higher than that of the Ni *d* levels. Thus the emission from the bottom of the band, where the Pd *d* levels are concentrated, is as strong as from the top although the density of Ni *d* states is actually higher in the top half of the band.

The results for NiPd suggest that the number of Ni *d* holes in the alloy is not decreased with respect to Ni, and may be increased, while the effective Ni bandwidth decreases. These are probably important factors in the existence of magnetism in Ni-Pd al-

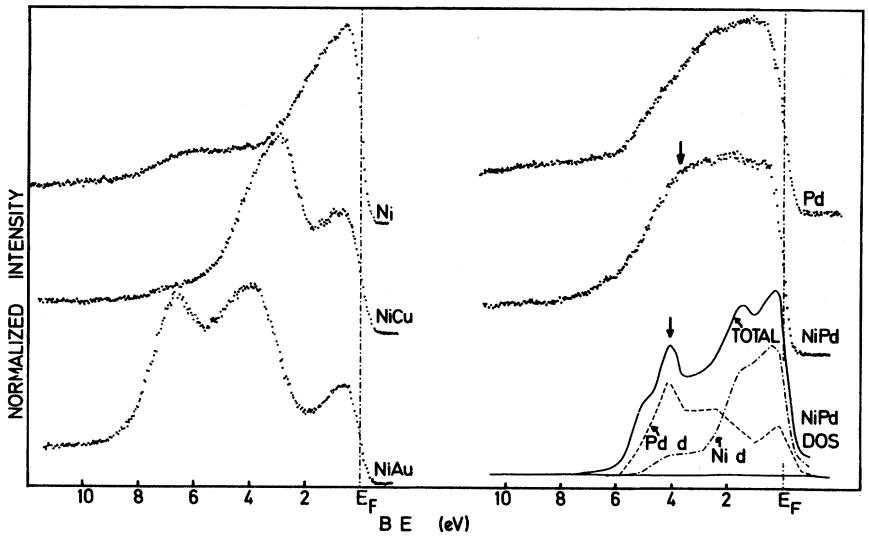

FIG. 8. XPS VB spectra from Ni, NiCu, NiAu, NiPd, and Pd. Calculated DOS curves are also shown for NiPd. For further explanation see text.

loys, even at Pd concentration as high as 98 at. %.[107,108] The observations are also important in determining satellite intensities, as discussed in paper II.

D. Ni alloys with La, Ce, and Th

The alloys of La, Ce, and Th are conveniently treated together because of the remarkable similarity of the La-Ni, Ce-Ni, and Th-Ni phase diagrams.[88,89,109] The spectra are shown in Figs. 9–11 and various parameters are listed in Table III. For the La-Ni and Th-Ni systems we also show the La and Th spectra normalized to the spectra of the most Ni-dilute intermetallics studied using La or Th core levels. Comparison of Figs. 9–11, and the data shown in Table III, both indicate strong similarities in the valence-band properties of La-Ni, Ce-Ni, and Th-Ni compounds with the same stoichiometry for all the alloys studied.

In both La_3Ni and Th_7Ni_3 a shoulder is observed

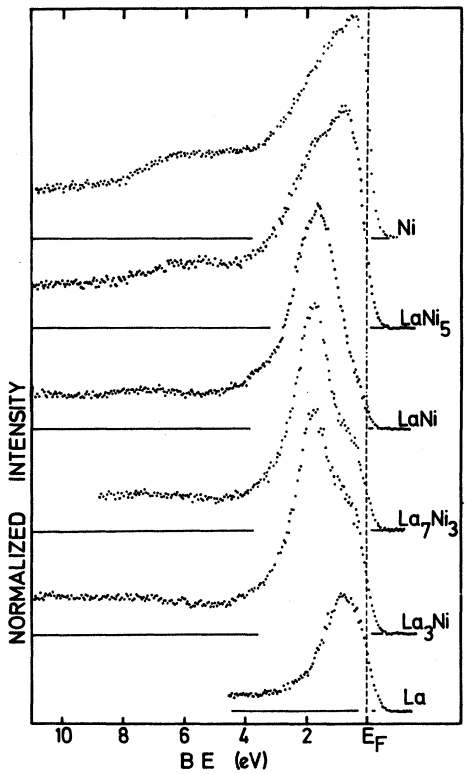

FIG. 9. XPS VB spectra from La-Ni alloys. All spectra have been normalized to the peak maxima, except for La. The La spectrum was normalized to the La_3Ni spectrum using the La $4d$ peaks (BE$\sim$100 eV), so that the area of the La contribution must be approximately the same in La_3Ni and La.

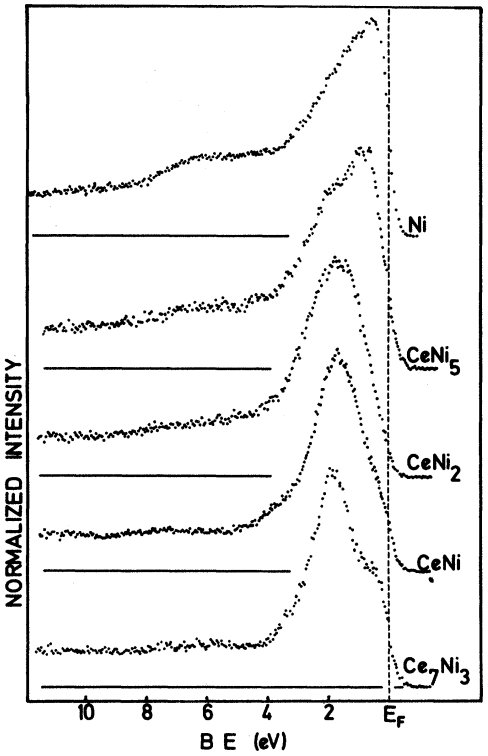

FIG. 10. XPS VB spectra from Ce-Ni alloys. All spectra have been normalized to the peak maxima.

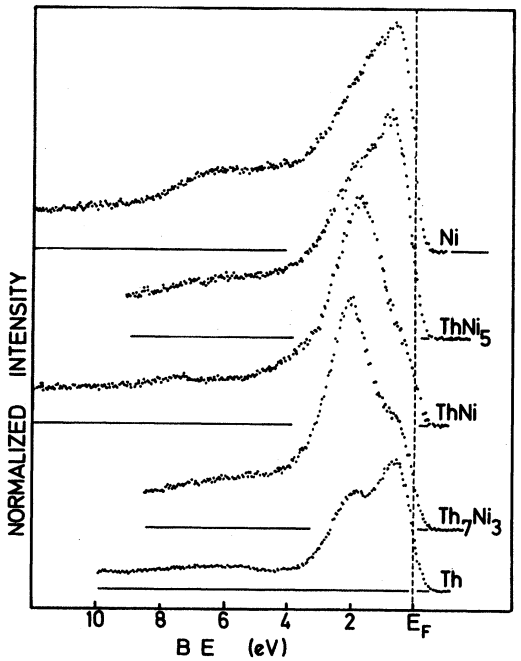

FIG. 11. XPS VB spectra from Th-Ni alloys. All spectra have been normalized to the peak maxima except for Th. The Th spectrum has been normalized to the Th_7Ni_3 spectrum using the Th $4f$ peaks (BE$\sim$333 eV).

TABLE III. Valence-band properties of La_xNi, Ce_xNi, and Th_xNi intermetallic compounds (all values in eV).

Material	Peak BE	±	Centroid BE	W^a	FWHM	Satellite BE	±
Ni	0.6	0.1	1.40	4.3	2.4	6.1	0.5
$LaNi_5$	0.85	0.2	1.50	3.7	2.4		
$CeNi_5$	0.85	0.2	1.35	3.75	2.4	6.4	0.5
$ThNi_5$	0.75	0.2	1.40	3.75	2.4	5.85	0.6
$CeNi_2$	1.60	0.2	1.65	3.6	2.1	7.0	0.8
LaNi	1.65	0.2	1.65	3.0	1.6	5.1	1.0
CeNi	1.60	0.2	1.70	2.8	1.8	6.5	1.0
ThNi	1.80	0.2	1.85	3.0	1.9	7.2	1.5
La_7Ni_3	1.6	0.2	1.80	2.1	1.4	6.7	1.0
Ce_7Ni_3	1.8	0.2	1.90	2.4	1.5		
Th_7Ni_3	1.9	0.2	2.00	2.6	1.5		
La_3Ni	1.65	0.2	1.90	2.1	1.4	7.4	0.5

[a]Determined as described in Appendix.

at E_F whose intensity is comparable to that in La and Th, respectively. This leads us to believe that the states at the Fermi level in these compounds have largely La or Th character, respectively, with the Ni d states being concentrated 1–3 eV below E_F. In all three systems we observe the shoulder at E_F to become relatively less intense as the Ni content is increased to 50% and the La, Ce, or Th content decreases. This is consistent with our view that the shoulders are due to states of largely La, Ce, or Th character.

As in all alloys of Ni with simple and transition metals, we observe that the Ni bands are only well separated from the Fermi level in Ni-dilute alloys. Table III quantifies the trends of the Ni d bands, which narrow and move to higher BE as the Ni content is decreased. The Ni d bandwidths in La_3Ni was the narrowest of all the alloys studied.

The Ni d^8-satellite intensity decreased strongly as the La, Ce, or Th intensity was increased. Although weak features are still found in the M_xNi alloys when $x > 1$, we believe there is not sufficient justification for assuming them to be Ni d^8 final states. Other effects, such as inelastic scattering losses, may offer alternative explanations.

The decrease of Ni d-state density at E_F on dilution with La, Ce, or Th receives support from low-temperature specific-heat measurements on $LaNi_5$ and $ThNi_5$ which showed the electronic specific heat to drop from 7.08 mJ g at.$^{-1}$ K^{-2} in Ni, to 6.38 and 6.08 mJ g at.$^{-1}$ K^{-2} in $ThNi_5$ and $LaNi_5$, respectively.[110,111] Although there are uncertainties in interpretation of the results due to electron-electron and electron-phonon interactions, the results are consistent with a decrease of 10–20% d-state density at E_F. We find E_F to shift only marginally to the low-intensity side of the midpoint of the photoemission onset at low BE in MNi_5 alloys (0.12±0.05 eV) but note that the *trend* with increasing La, Ce, or Th concentration supports the notion of Ni d-state density decrease at E_F in the MNi_5 alloys with respect to Ni.

We know of only one DOS calculation relevant to these alloys, that for the YNi_2 by Cyrot and Lavagna.[112] Our experience is that there is little difference between the Ni or Pd d-band characteristics of Sc, Y, La, Ce, and Th alloys. Cyrot and Lavagna found the Ni d bands to be centered about 0.22 Ry (2.8 eV) below E_F while we find only 1.65 eV in $CeNi_2$. Cyrot *et al.* put the top of the d band at about 1.3 Ry (1.7 eV) while we find the top to be only just below E_F. Their calculated width (2.5 eV) is comparable with ours when one takes experimental and lifetime broadening into account. Their observation that YNi_2 is a Pauli paramagnet[112] and other observations that Ni does not carry any 3d magnetic moment in RNi_2 compounds[113–115] is consistent with the very low density of Ni d states at E_F which we find in $CeNi_2$.

E. Aluminum-palladium alloys

Aluminum is soluble to about 14 at. % in palladium at 300 K, and in addition two congruently melt-

TABLE IV. Pd *d*-band properties in Pd alloys (all values in eV).

Material	First peak BE	±	Second peak BE	±	Third peak BE	±	Centroid BE	W^f	FWHM
Pd	0.95	0.2					2.3	5.9	4.1
$Al_{10}Pd_{90}$	1.4	0.2					2.3	6.0	4.1
AlPd	3.6	0.2	4.6	0.2			4.1	4.6	3.1
Al_3Pd	4.8	0.2					4.8	3.2	1.8
ScPd	3.6	0.2					3.6	4.2	2.8
ScPd[a]	3.5		4.3					3.1	2.1
$TiPd_3$	1.0	0.4	2.1	0.2	4.2	0.4	2.8	6.2	4.4
VPd_3	1.0	0.3	2.1	0.2	4.3	0.4	2.8	6.2	4.4
VPd_2	2.5	0.2	4.4	0.3			3.3	5.6	3.8
VPd	2.8	0.2	4.2	0.3			3.6	5.1	3.8
V_3Pd	2.4	0.4	4.0	0.3			3.9	4.4	3.3
NiPd[e]	~0.7	0.3	2.0	0.5	4.0	0.5	~2.3	~6.2	~5
YPd_3	1.0	0.3	2.1	0.2	3.9	0.3	2.6	5.4	3.8
Y_7Pd_3	3.8	0.2					3.8	2.5	1.5
$ZrPd_3$[b]	2.8		3.9					5.6	4.0
ZrPd[b]	3.7							4.8	3.3
Zr_2Pd[b]	3.8							3.2	2.6
Zr_3Pd[c]	3.5								
$NbPd_2$	2.8	0.2	4.5	0.3			3.0	5.7	~3.8
Pd_3Ag_{70}[d]	1.8						~1.8		
$TaPd_3$			2.7	0.3	5.1	0.5	3.1	6.4	4.5
$TaPd_2$			3.0	0.3			3.6	5.5	~4
TaPd			3.55	0.3			3.8	5.3	3.1

[a]Ultraviolet photoemission spectroscopy (UPS) from Ref. 122.
[b]Reference 40.
[c]Reference 37.
[d]Reference 167.

ing (AlPd and $AlPd_2$) and two peritectic alloys can be formed (Al_3Pd and Al_3Pd_2).[79,82] In Fig. 12 we illustrate the behavior of the XPS valence bands with spectra of one solid solution ($Al_{0.1}Pd_{0.9}$), the congruently melting AlPd and the peritectically melting Al_3Pd. The most important valence-band parameters are listed in Table IV. The differences between $Al_{0.1}Pd_{0.9}$ and Pd are subtle: In the alloy there is a slight increase in relative intensity of 1.6 eV below E_F. Also the midpoint of the rise in intensity at the top of the band is ~180 meV below E_F. As the resolution of these measurements was only 600 meV we cannot say how low the DOS at E_F is, but it is certainly considerably lower than in Pd itself. This is in qualitative agreement with the observation that the low-temperature specific heat of $Al_{0.1}Pd_{0.9}$ is about half that of Pd (Ref. 116) and with observations of the magnetic susceptibility of Al-Pd alloys with low Al content.[117]

Pd has ~0.36 holes per atom in its *d* band.[118]

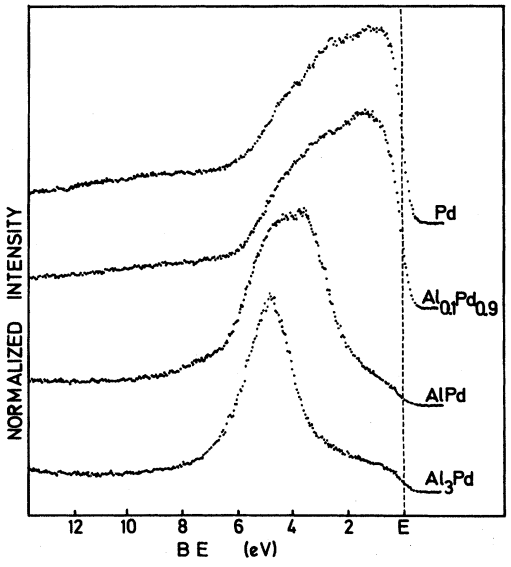

FIG. 12. XPS VB spectra from Pd, $Al_{0.1}Pd_{0.9}$, AlPd, and Al_3Pd.

Glugla *et al.*[116] have argued that Al contributes between 2.6 and 3 electrons per Al atom to the Pd conduction band, so that the Pd *d* band would be full at about 10—15 at. % Al which is close to the 14% limit of solid solubility of Al in Pd at 300 K. Our XPS results in Fig. 12 also indicate that there is a strong tendency for Al to fill the Pd band. Our calculations for AlPd and Al_3Pd indicate that there is always Pd *d* character in the bands above E_F, which is further evidence that Al does not have to donate an unrealistically large charge transfer to the Pd sites in filling the Pd *d* band. The band filling takes place by hybridization of the Al *s* and Pd *d* states.

In the two ordered alloys the main peaks are attributed to Pd *d* states which have a large cross section. The movement of the Pd *d* band to higher BE and their narrowing with increasing Al content is far stronger than the effect on the Ni 3*d* bands in the corresponding Ni alloys (see Tables II and III). We have made a comparison of the calculated total DOS's for AlPd in its high-temperature CsCl structure and Al_3Pd in a Cu_3Au structure with the experimental XPS spectra in Fig. 13. The calculated DOS's, as well as the XPS spectra are dominated by the Pd 4*d* states. However, the positions of the peaks are not well reproduced by the calculations as seen in the upper half of Fig. 13, and the centroids of the calculated peaks are approximately 0.4 eV deeper than experiment for AlPd and 0.6 eV shallower in Al_3Pd. As in other cases the discrepancies can be attributed to the effects of hole creation, matrix-element effects, or problems in comparison of band-structure calculations with experiment, or a combination of these effects. In the case of Al-Pd alloys we can attempt to narrow down the possibilities as described below.

When a *d* resonance is placed in an *s* band the *s*-state density exhibits a minimum at, or just above, the *d*-resonance energy and a maximum to the high BE side of the *d* resonance (see, e.g., Refs. 33, 34, 119, and 120). The position of this *s*-band maximum is closely connected with the position of the *d* resonance or band, and any problems with the theoretical scheme must affect both *d* and *s* peaks. The Al $L_{2,3}$ x-ray spectra probe the densities of *s* and *d* states because of dipole-selection rules and are dominated by the *aluminum* states because the matrix elements are highly localized. We chose to do the calculations on AlPd and Al_3 Pd because the Al $L_{2,3}$ x-ray spectra are available.[121] The calculated densities of Al *s* states are compared with the observed x-ray spectra in the lower half of Fig. 13. The experimental spectra have significant plateaus in the region 0—5 eV which we attribute to "cross transitions" to the Pd *d* states and Al *d* states. Neither of these effects is very important at BE > 5 eV, where the intensity is attributed to Al *s* states. The general structures of the spectra are much broader than those of the calculation and this is not explicable in terms of instrumental or core-level lifetime broadening as these total only 0.3 eV. A possible

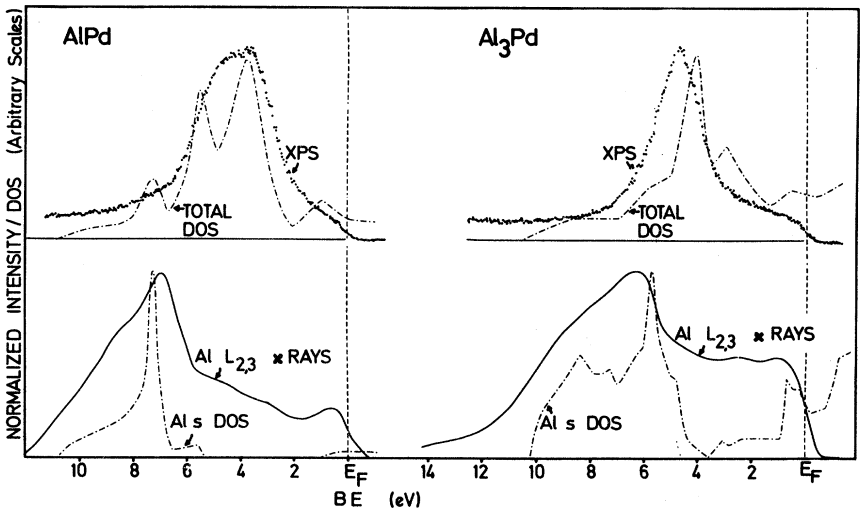

FIG. 13. Upper half: Comparison of calculated total DOS curves (broadened by a 0.6-eV Gaussian function) with XPS spectra for AlPd and Al_3Pd. Lower half: Comparison of Al $L_{2,3}$ x-ray-emission spectra and calculated densities of Al *s* states for AlPd and Al_3Pd.

explanation is lifetime broadening of the final states with a hole in the valence bands, which is known to be as large as 2 eV in some cases, and to vary with position in the band.[12,13,15] Despite the broadening, the shape of the x-ray spectra do resemble the calculated densities of Al s states. However, the calculated Al s peaks are $\sim$0.4 eV too deep in AlPd and $\sim$0.6 eV too shallow in Al_3Pd. It is true that a calculation including x-ray-emission matrix elements and lifetime broadening is desirable, but we can judge the effects of these two factors from other systems that have been studied.[101,102] It is unlikely that the two factors could lead to the shifts between calculation and experiment described by Fig. 13.

Summarizing the lessons of Fig. 13 we may say that the calculated Al s- band Pd d-band positions are both 0.4 eV deeper than experiment in AlPd and are both 0.6 eV shallower in Al_3Pd (within an experimental accuracy of $\sim$0.2 eV). The cross sections for Al ($2p \leftarrow 3s$) x-ray emission and Pd d photoemission may vary with position in the respective bands, but it is unrealistic to suggest that the variations can lead to the same shifts in two very different bands examined by two very different spectroscopies. We will return to the consequences of these observations in Sec. V E.

F. Pd alloys with transition metals

There have been several reports on photoelectron spectra from Pd alloys with early transition metals such as Sc (Ref. 122) and Zr.[37–40] All these studies indicated a large shift of the Pd bands to higher BE upon alloying. An early suggestion that this was a special characteristic of glassy alloys[37] has now been convincingly disproved.[40] In this section we report the XPS valence bands of V-Pd and Ta-Pd alloys which are reproduced in Figs. 14 and 15 and also discuss new data from ScPd, Y_7Pd_3, and $NbPd_2$ (see Tables IV and V), YPd_3 and $TiPd_3$ (Fig. 19).

In the case of vanadium-palladium alloys we calculated the total DOS for VPd_3, and V_3Pd (Ref. 123) shown in Fig. 14. When we projected out the V and Pd d states separately it became clear that the peaks in the total DOS which straddle E_F are due to states centered mainly on the V sites, but with a small contribution even above E_F centered on the Pd sites. Comparison with theory, and the knowledge that the cross section for Pd electrons is larger than for electrons with mainly V d character (Table I) allows us to assign the main XPS emission to Pd d states. In these and other Pd alloys, the

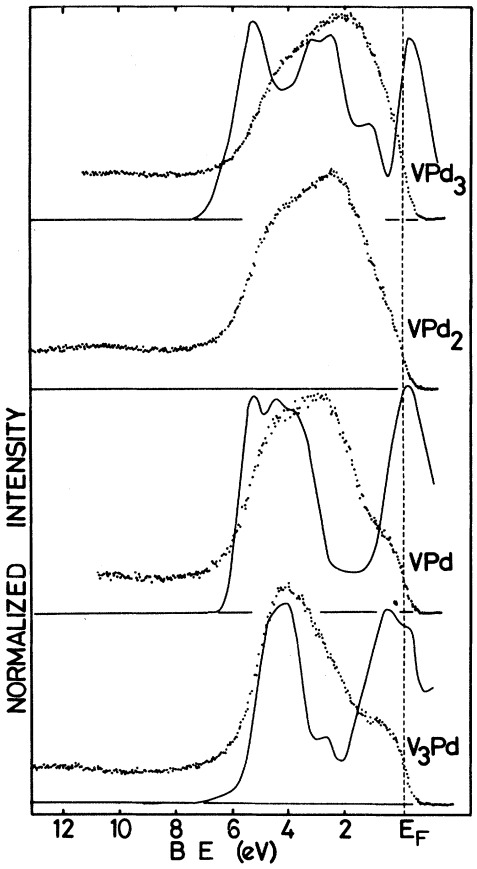

FIG. 14. XPS VB spectra of VPd_3, VPd_2, VPd, and V_3Pd. The calculated total DOS curves for VPd_3, VPd, and V_3Pd have been broadened by a 0.6-eV Gaussian function, roughly normalized to the XPS intensities and plotted as full lines.

XPS spectra often show partially resolved peaks and shoulders in the Pd d bands whose BE's are listed in Tables IV and V along with the centroids, as defined by the methods described in the appendix. As the V concentration is increased a shoulder at E_F becomes visible in the XPS spectra and can be attributed to the states with mainly V d character.

The strong drop in XPS intensity at E_F between Pd and VPd_3 is in keeping with the threefold decrease in electronic specific heat as up to 10 at. % of V is dissolved in Pd (Ref. 124) and indicates that the Pd band is rapidly filled by V admixture. The same effect is postulated on the basis of vanadium appearance potential results.[125] It has been argued that the "valence" of V in a Pd host is about 3, i.e., that each V atom "donates" about three electrons to the Pd band.[124,125] The results of our calculations indicate that in VPd_3, VPd, and V_3Pd there is al-

TABLE V. Pd *d*-band properties in Pd alloys with Y, lanthanides, Th, and U (all values in eV).

Material	First peak BE	±	Second peak BE	±	Third peak BE	±	Centroid	W^a	FWHM
Pd	0.95	0.2					2.3	5.9	4.1
YPd_3	1.0	0.3	2.1	0.2	3.9	0.3	2.6	5.4	3.8
$LaPd_3$			2.2	0.2	3.7	0.3	2.5	5.1	3.2
$CePd_3$	1.3	0.3	2.65	0.2	4.0	0.3	3.1	5.5	3.7
$PrPd_3$			2.6	0.2	3.9	0.3	2.8	5.4	3.6
$NdPd_3$			2.2	0.2	3.9	0.3	2.8	5.1	3.8
$SmPd_3$			2.6	0.2	3.8	0.3	2.8	5.4	3.6
$ThPd_3$	1.9	0.3	3.2	0.2	4.8	0.3	3.5	5.2	3.4
UPd_3	1.7	0.3	3.1	0.2	4.9	0.3	3.6	5.2	3.6
$LaPd_2$	3.3	0.3					3.3	4.2	2.9
Ce_3Pd_5	3.4	0.3					3.4	4.1	3.0
LaPd	3.3	0.2					3.5	3.4	2.2
CePd	3.3	0.2					3.3	4.1	2.9
ThPd	3.9	0.2					3.9	3.8	2.5
Y_7Pd_3	3.8	0.2					3.8	2.5	1.5
La_7Pd_3	3.5	0.2					3.5	2.3	1.4
Ce_7Pd_3	3.7	0.2					3.7	2.4	1.4
Th_2Pd	3.9	0.2					4.0	3.0	1.8
LaPdAl	3.75	0.2					3.8	2.8	1.6
CePdAl	3.75	0.2					3.8	3.0	1.8
ThPdAl	4.0	0.2					4.0	3.3	2.0

[a]Determined as described in Appendix.

ways some Pd character in the unoccupied V *d* bands and some V *d* character in the occupied Pd *d* bands. We do not wish to attach a number to the quantity of unoccupied Pd *d* character because of the ambiguity of defining the boundaries of the Pd atoms. However, the total unoccupied Pd *d* character per Pd atom is nearly constant in Pd and V-Pd alloys so that the filling of the Pd *d* bands is definitely dominated by mixing of the V and Pd states.

The XPS spectra of Ta-Pd alloys, reproduced in Fig. 15, are similar to those of V-Pd alloys of the same stoichiometry, although the Pd *d* bands are typically shifted 0.3 eV to higher BE in the Ta alloys (Table IV). As in the V alloys, the Pd bands move away from E_F with increasing Ta content. The shoulder at E_F due to V or Ta *d* bands, in alloys of higher Ta content is more marked in the Ta alloys. This is at least partly explained by the higher cross section of Ta *d* electrons with respect to V *d* electrons. The Ta spectrum shown in Fig. 15 has been normalized to the TaPd spectrum using a Ta core level. Its intensity is slightly lower than the shoulder in TaPd, which could be related to narrowing of the Ta bands in TaPd or to the presence of some Pd character in the levels at E_F.

The Nb-Pd phase diagram is different from that of Ta-Pd, which is surprising in view of the normally extreme similarity in the chemistry of Nb and Ta. The phase diagram is also rather ill defined[126] and we only succeeded in preparing $NbPd_2$ as a single phase. All attempts to prepare the other metalloid listed (Nb_3Pd_2) gave a product with several phases. The spectrum of $NbPd_2$ (not shown) was similar to that of $TaPd_2$ and clearly showed a shoulder at E_F which we attribute to states of mainly Nb character. As in the corresponding V and Ta alloys the Pd band appeared to be filled and to start some way below E_F. It is interesting that a single monolayer of Pd on a Nb substrate also has no Pd *d* states at E_F and is inactive as a catalyst for H uptake.[127,128] The implication of that surface study for our work is that the surface chemical activity of the Pd atoms will be strongly modified in those of our alloys where there are no Pd *d* states at E_F.

The spectra of YPd_3, $TiPd_3$, and VPd_3 can be compared (see Fig. 19), as can their peak positions (see Tables IV and V). In the Ti-Pd phase diagram there is positive deviation of the melting point at

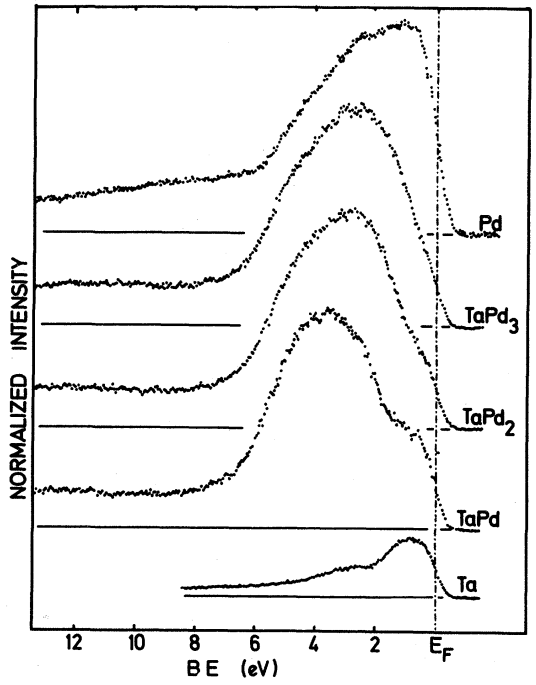

FIG. 15. XPS VB spectra from Ta-Pd alloys. All spectra have been normalized to the maximum VB intensity, except that of Ta, which has been normalized to the TaPd spectrum using the Ta $4f_{7/2}$ peak with BE$\sim$22 eV.

the $TiPd_3$ composition, indicating a high heat of formation, whereas VPd_3 is only stable at low temperatures. ($CrPd_3$ does not form at all.) Despite this difference in stability of $TiPd_3$ and VPd_3 we see no major differences in the XPS spectra. Both spectra indicate a density of Pd d states at E_F which is smaller than in Pd. There are distinct differences between the spectra of $TiPd_3$ or VPd_3 and that of YPd_3, where the Pd d bands are further from E_F. In this respect Y is like the rare earths which are very effective at filling the Pd d bands and driving the Pd d bands to higher BE's, away from E_F. The results for ScPd indicate that Sc is similar to Y in its effect on Pd d bands. The results of Steiner *et al.*[40] indicate that Zr is intermediate between Y and Nb or Ta.

The calculations tend to overestimate the experimental separation of the Pd and V d bands. This effect is discussed further in Sec. V E. In VPd_3 the calculated DOS has much stronger structure than experiment. This is thought to be largely due to lifetime broadening in the final state, which tends to be larger for the states at the bottom of the d bands (see, e.g., Ref. 15). In addition states at the bottom of the band have "bonding" character which causes them to have greater density between the atoms.[100,101,123] This increase in the expectation radius leads to a lower photoelectron cross section. When the shift, lifetime broadening, and energy dependence of cross section are all taken into account the shape of the VPd_3 XPS spectrum is reasonably well explained by the calculated DOS curve. In VPd and V_3Pd the calculated Pd d bands are at higher BE than in experiment but they are also much narrower. Visual inspection of the spectra shows that they could not be *readily* reproduced just by Lorentzian (lifetime) broadening of the theoretical curve. One explanation for the large experimental broadening is random occupation of the lattice sites; V_3Pd has the random β-W (WO_3) structure.[83] The contribution to bandwidth from Pd-Pd interactions is proportional to the number of Pd-Pd nearest-neighbor interactions, and if this is not constant we must expect broadening of the spectra due to different environments for the Pd atoms. This effect is not included in the calculations where the ordered Cu_3Au and CsCl structures were used and although other factors may contribute to the experimental bandwidths it is not sensible to seek them here.

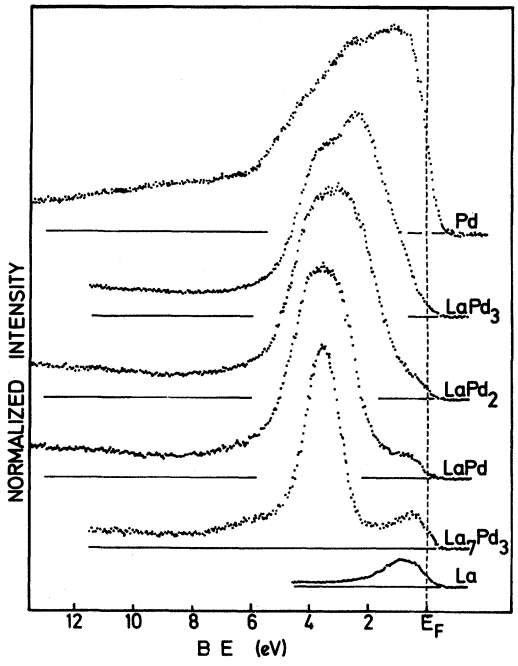

FIG. 16. XPS VB spectra from La-Pd alloys. All spectra have been normalized to the maximum VB intensity, except that of La which has been normalized to the La_7Pd_3 spectrum using the La $4d$ peaks at BE$\sim$100 eV.

G. Alloys of rare earths and actinides with Pd

There are strong similarities of the phase diagrams of Pd with Y, La and the lanthanides, Th, and U. We thus treat these alloys together. The spectra for La-Pd, Ce-Pd, and Th-Pd alloys are reproduced in Figs. 16—18 and some data is included in Table V. In all these spectra the contribution of the La, Ce, or Th states is small. This is illustrated in Figs. 16 and 18 by the La and Th spectra which have been normalized with core levels to the same scale as La_7Pd_3 and Th_2Pd, respectively. The area in the La and Th spectra is thus approximately equal to the area of the La and Th contributions to the La_7Pd_3 and Th_2Pd spectra. The La and Th spectra strongly resemble the small peaks at E_F in La_7Pd_3 and the Th_2Pd in both shape and intensity. This leads us to assign the shoulders and peaks near E_F in all the La-, Ce-, or Th-rich alloys with palladium to states with largely La, Ce, or Th character. The decrease in relative intensity of these shoulders with increasing Pd content supports our assignment.

In the Pd alloys, as in the Ni alloys, the Pd *d* bands are centered at much higher energies and are much narrower in the La-, Ce-, or Th-rich alloys. Comparison with the transition-metal alloys, e.g., the V- or Ta-Pd alloys in Figs. 14 or 15, will convince the reader that this narrowing is much stronger in the La, Ce, and Th alloys. Although the similarities between the *trends* in La-, Ce-, or Th-Pd alloys are pronounced, closer examination reveals significant differences. One example is the width of the Pd bands in CePd which is ~0.7 eV larger than in LaPd or ThPd. Another example is the absence of a minimum between the Ce and Pd bands in Ce_7Pd_3, which is found in both La_7Pd_3 and $ThPd_2$. Also the Ce-Pd phase diagram is exceptional among the *R*-Pd diagrams in that it has no stable $CePd_2$ phase, the nearest being Ce_3Pd_5. In all these cases we tentatively attribute these differences to the Ce $4f$ level. In separate studies we have found strong indications for mixing of the Ce $4f$ levels with Ni or Pd states.[129,130] The intensity of the photoemission from the Ce $4f$ level is seldom sufficient to perturb the XPS spectra significantly.[66,131—133] However, their hybridization with the Pd levels could distort the Pd bands enough to give significant changes in the XPS spectra.

We have examined a wide range of MPd_3 alloys and reproduce many of the spectra in Fig. 19. Almost all of the emission comes from the Pd $4d$ lev-

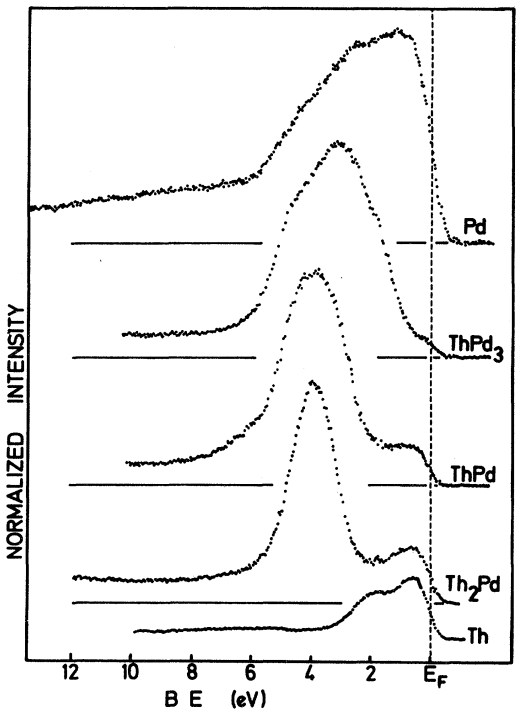

FIG. 18. XPS VB spectra from Th-Pd alloys. All spectra have been normalized to the peak VB intensity, except that of Th which was normalized to the Th_2Pd spectrum using the Th $4f_{7/2}$ peak at BE ~ 333 eV.

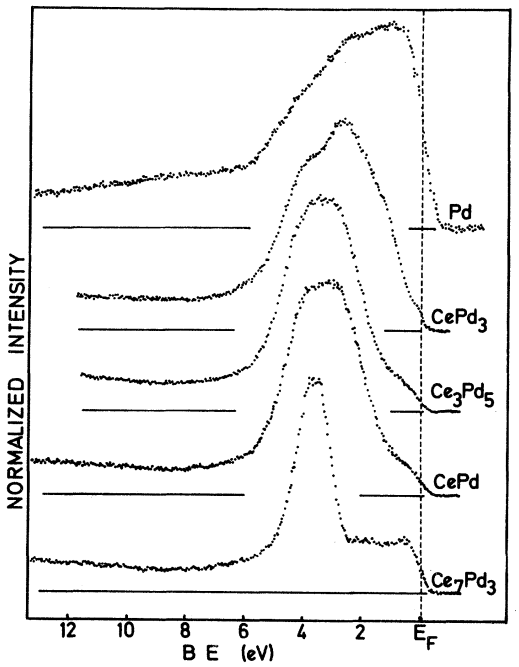

FIG. 17. XPS VB spectra from Ce-Pd alloys.

els: The *approximate* proportions of emission from levels of the second component, in percent, calculated from Scofield tables[66] are as follows: Ti=1, V=2, Y=1.7, La=2, Ce=3, Pr=8, Nd=12, Sm=20, Th=2.5, and U=19. In $CePd_3$ and UPd_3 the $4f$ and $5f$ levels are observed as shoulders at E_F.[133,134] In the alloys with Ti, V, Y, La, and Th the emission from the second component does not visibly affect the spectrum, while in the alloys with Pr, Nd, and Sm the rare-earth $4f$ emission lies in the Pd $4d$ bands and only leads to a distortion of the $4d$ peaks. The shape of the YPd_3 spectrum with a maximum at 1.2 eV and broad shoulders at $\sim$1.0 and $\sim$3.9 eV, corresponds well to the calculated DOS which has its main maximum at $\sim$2.0 eV, a shoulder at $\sim$0.6 eV, and a second peak at $\sim$3.7 eV. We were surprised to find significant differences between the spectra of YPd_3 and the rare-earth Pd_3 alloys because these elements are normally considered so similar. However, the Pd $4d$ bands of $CePd_3$ are deeper than in YPd_3 or $LaPd_3$, and the low-energy shoulder at 1–1.3 eV is far less pronounced in $LaPd_3$, $NdPd_3$, $PrPd_3$, and $SmPd_3$ than in YPd_3 or $CePd_3$. The differences between $CePd_3$ and the others can be attributed to the influence of the Ce $4f$ level, but the reason for the other differences is not clear to us at present.

Comparison of the spectra of $ThPd_3$ and UPd_3 is interesting because all the features are so similar, except for the shoulder at E_F in the UPd_3 spectrum. Its approximate area is shown in Fig. 19 and is attributed to the U $5f$ levels. The features deeper in the band are thought to originate from the same three-peak structure of the Pd $4d$ levels found in YPd_3. It is notable that the three features are nearly 1 eV deeper in $ThPd_3$ and UPd_3 than in YPd_3 (see Fig. 19 and Table IV) and over 0.5 below their values in $CePd_3$. These differences are larger than found in the other alloys of the same stoichiometry when M=Y, La, Ce, or Th. Less notable, although still experimentally significant, was the fact that the binding energies of the Pd $4d$ levels in Th compounds were larger than those of Y, La, or Ce compounds in all stoichiometries studied.

H. Valence bands of LaPdAl, CePdAl, and ThPdAl

The observed valence-band spectra of these three compounds are reproduced in Fig. 20 All three have rather narrow Pd d-band peaks with widths of about 3 eV and centroid binding energies of 3.8–4 eV. The valence bands are not consistent with a mixture of binary phases such as M_7Pd_3, MPd, AlPd, and Al_3Pd where M=La, Ce, or Th (for Th phases Th_2Pd would be appropriate as Th_7Pd_3 does not exist). The binding energies for these ternary compounds, listed in Table IV are intermediate between those for the 1:1 LaPd, CePd, or ThPd com-

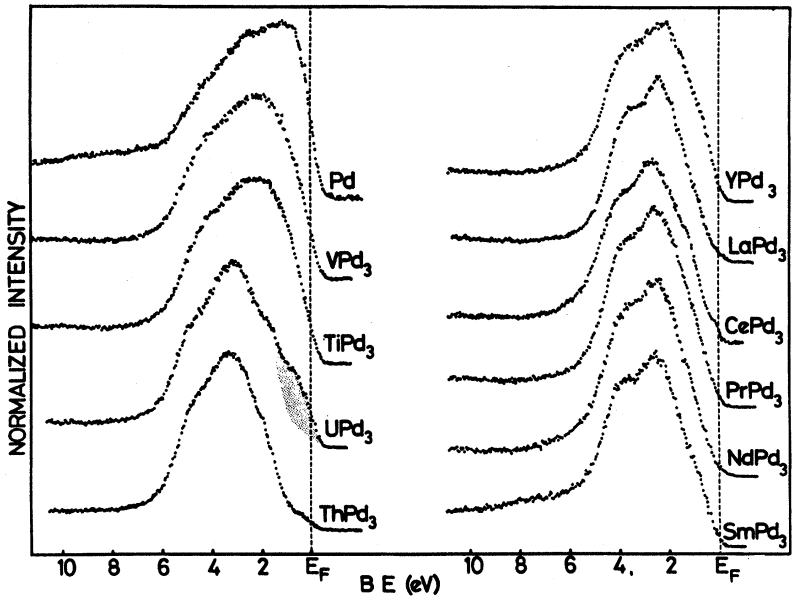

FIG. 19. XPS VB spectra from MPd$_3$ alloys. The approximate area attributed to the U $5f$ levels in UPd_3 has been shaded. Also shown as full lines are the computed, full DOS curves for $TiPd_3$ and YPd_3.

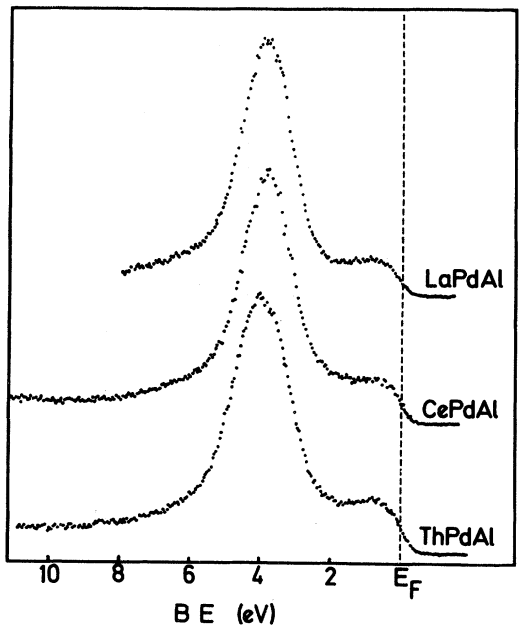

FIG. 20. XPS VB's of LaPdAl, CePdAl, and ThPdAl.

pounds and AlPd. Whatever the mechanism for the Pd VB shifts, the effects of La, Ce, or Th, and Al are clearly not simply additive.

V. DISCUSSION

A. d^8 satellite

Before dealing with the observations on the valence-band properties themselves we will dispose of points concerning the d^8 valence-band satellite. The Ni d^8 satellites get weaker in alloys with electropositive elements as the Ni d band is filled. It is, however, difficult to quantify this weakening because of inelastic scattering and the creation of electron-hole pairs in the excitation of the valence-band spectrum.[135,136] In the Pd-alloy VB spectra the difficulty is even more marked. There is a high background at high BE, below the valence band in Pd itself and this does decrease in Pd alloys with electropositive metals. Nevertheless as there is no well-defined satellite in the background we do not insist that d^8 final states are important in the XPS spectra of Pd and its alloys. For Ni alloys, trends in VB satellite intensity parallel those found in Ni core-level peaks where, as reported in paper II, quantification is easier. We discuss the implications of trends in satellite intensity and band filling in paper II where core levels are treated.

Johannsson *et al.*[17] have noted that the binding energy of the valence-band satellite in Ni was numerically identical to the two-electron binding energy of the VV final state derived from MVV and LVV Auger peaks. Here M and L were either $3p$ or $2p$ core holes and V represented a hole in the $3d$ valence band. In Table VI we have compared the valence-band satellite energies for Ni and the 12 Ni alloys with well-defined satellite, to the corresponding two-electron binding energies derived from the L_3VV Auger transition from paper III. Within experimental accuracy there is good agreement. The satellite energy is not constant, but changes by as much as 1.6 eV with similar changes in the Auger-derived two-electron BE. Note that there are five

TABLE VI. Comparison of $2e^-$ BE's of the XPS VB satellites and the ^1G d^8 term from Auger spectroscopy (from paper III; all values in eV).

Material	$2e^-$ BE (satellite)	±	$2e^-$ BE (^1G Auger)
Ni	6.1	0.5	6.45
$MgNi_2$	6.7	0.5	7.05
Mg_2Ni	6.7	0.5	6.90
$AlNi_3$	6.7	0.5	6.85
AlNi	7.7	0.5	7.50
ScNi	7.1	0.5	6.85
TiNi	7.2	0.5	7.45
$CrNi_2$	6.8	0.5	7.05
InNi	6.6	0.5	6.45
$TaNi_3$	6.5	0.5	6.85
$TaNi_2$	7.7	0.5	7.55
$CeNi_5$	6.4	0.6	6.45
$CeNi_2$	7.0	0.8	7.00

possible multiplet configurations for d^8 atoms.[137] The ^1G configuration dominates the Auger spectrum, but as we report in paper III, under certain circumstances a peak at ~ 2 eV lower BE than the ^1G can be resolved and is attributed to the ^3F term. The results in Table VI are in agreement with the results of a calculation by Davis *et al.*[138] which suggested that the ^1G final state is the most important for the d^8 satellite. In many of the spectra there is no minimum between the satellite and the VB, so the satellite looks like a long plateau. This may be an indication that other d^8 final states are important in the satellite, for instance the ^3F final state. This idea was born out in the calculations of Davis for Ni. Unfortunately even in Auger spectra the ^3F term can only be resolved in a few Ni alloys where the Ni bands are full and the satellite is weak.

B. Widths of Ni and Pd *d* bands in alloys

The widths of the Ni and Pd *d* bands decrease markedly in the alloys with electropositive metals studied here. The trend is more noticeable in the Pd alloys because the Pd bands are broader than the Ni bands in the pure element. However, the widths in lanthanide alloys with low Ni or Pd concentration are very similar, as in Ce_7Ni_3 and Ce_7Pd_3, for example. In all cases, the Ni and Pd *d*-band width decreased with decreasing Ni and Pd concentration. We are of the opinion that the stoichiometry and electronegativity are the most important factors in our observations but we must discuss other effects and the mechanism of electronegativity effects.

The bandwidths can be analyzed in terms of the following:

(1) Lifetime effects on the final-state hole.
(2) Spin-orbit splitting.
(3) Variation of interatomic distances and extension of the wave functions.
(4) Variation of number of Ni-Ni or Pd-Pd nearest-neighbor contacts.
(5) Hybridization with the bands of the partner atoms.
(6) Interaction between Ni or Pd atoms via the intermediate atoms of the second metal.

Lifetime effects lead to a Lorentzian broadening of the bands. They could be significant in the dilute Ni and Pd alloys where the bands have a sharp peak and wide base but in no case here have we observed peaks with long tails and the shape expected if there were a very large Lorentzian contribution to the shape.

Spin-orbit coupling effects are larger in Pd than Ni, but even here the *maximum* observed splitting of the bands in pure Pd was only ~ 0.4 eV.[139] Such effects are not large enough to strongly affect our data.

Concerning the effect of variation of interatomic distances, Andersen has shown that the interatomic *d*-hopping integrals and hence the *d*-band widths of metallic elements are inversely proportional to the fifth power of the distance between the atoms.[71,140,141] This result is valid for all distances in the absence of hybridization and should give a correct indication of the trends in Ni-Ni or Pd-Pd hopping. Watson *et al.* quote dependence between $r^{-3.2}$ and r^{-5} for transition metals.[57] This reduction is presumably due to hybridization. Such rules imply that we need only consider nearest-neighbor interactions here. Another rule which is often applied is that in the tight-binding approximation, and for a given atomic distance, the bandwidth is proportional to the coordination number. In order to apply these rules to the alloys studied, we must consider the individual crystal structures of the alloys and the Ni-Ni or Pd-Pd nearest-neighbor interactions which are given in Tables VII and VIII. Unfortunately we cannot always give these details because in some of the crystal structures of low symmetry the positions of the atoms in the unit cells are not given by the lattice constants alone. Nevertheless some definite points emerge.

Consider the cases of Ni, ScNi, and TiNi. The number of direct Ni-Ni contacts drops from 12 in the element to six in the intermetallics, which leads us to expect a factor of 2 decrease in Ni *d*-band width on the basis of the above arguments. The Ni-Ni distance has also increased by a factor of $\sim 20\%$ in the intermetallics so that even if the bandwidth was proportional to only the third power of $1/r$ (Ni-Ni) we would expect the Ni *d* widths to decrease by another factor of 2. In contrast to these expectations, Table IV shows the Ni *d*-band widths in TiNi and ScNi to be only $12-25\%$ smaller than in Ni. The correlation effects which narrow the pure-Ni spectrum[12–15] and the instrumental broadening of 0.6 eV play a small role in reducing the change in W between Ni and ScNi or TiNi. However, they cannot explain why the change is *so* small. The observed results indicate that the number and distances of Ni-Ni contacts cannot, by themselves, explain the observed Ni *d*-band widths, which is not an unexpected result. Another example of such effects is given by alloys like V_3Pd,

TABLE VII. Structures and Ni-Ni distances in Ni alloys. (N.B. The positions of atoms in unit cells with free coordinates are not always well defined; some of the interatomic distances given here were determined by analogy with more completely characterized compounds of a similar structural type.)

Compound		Structure type	r_1 Ni-Ni	CN	r_2 Ni-Ni	CN	References
Ni		*A*1	2.49	12			82, pp. 119,148
$MgNi_2$		$MgNi_2$	2.40	4	2.96	4	80, p. 910
Mg_2Ni		Mg_2Ni	2.60	2			80, p. 910; 82, pp. 119,1 85, pp. 15,95
$AlNi_3$		Cu_3Au	2.53	8			80, p. 48; 85, pp. 30A,106
AlNi		CsCl	2.83	6			79, p. 121; 81, p. 32
Al_3Ni		Al_3Ni	2.74	3			82, pp. 127,164; 83, p. 1
Al_3Ni		Al_3Ni					79, p. 121; 83, p. 105
ScNi		CsCl	3.15	6			81, pp. 121,148
TiNi		CsCl	~2.99	6			85, pp. 13,91
$CrNi_2$		?	?	?	?	?	81, p. 273
CuNi		random Ni	2.60	~6			
InNi	HT	CsCl	3.09	6			79, p. 854
	LT	CoSn	2.61	4			79, p. 854; 85, pp. 9,91
NiPd		solid solution Ni	2.64	~6			83, p. 782
$LaNi_5$	$3\times Ni_A$	$CaCu_5$	2.48	4	2.46	4	80, p. 572; 85, pp. 11,59
	$2\times Ni_B$		2.46	6	2.88	3	
LaNi		CrB	2.55	2			86, pp. 9,28
La_7Ni_3		Th_7Fe_3		0			86, p. 8
La_3Ni		Fe_3C		0			79, p. 887; 83, p. 105
$CeNi_5$	$3\times Ni_A$	Cu_5Ca	2.44	4	2.45	4	79, p. 303
	$2\times Ni_B$		2.45	6	2.81	3	
$CeNi_2$		Cu_2Mg	2.55	6			79, p. 303
CeNi		CrB	2.65	2			85, pp. 26,109
Ce_7Ni_3		Th_7Fe_3		0			79, p. 303; 85, pp. 26,108
$TaNi_3$		Cu_3Ti	2.60	4	2.67	4	79, p. 674; 85, pp. 29,127
$TaNi_2$		$MoSi_2$	2.59	4	2.63	1	81, p. 558; 85, pp. 29,69
TaNi	$6\times Ni_A$	W_6Fe_7	2.46	4	2.49	$\sim\frac{1}{2}$	81, p. 558
	$\sim\frac{1}{2}Ni_B$		2.49	6			
Ta_2Ni		$CuAl_2$	2.44	2			81, p. 558
AuNi		solid solution Ni	2.72	~6			83, p. 438
$ThNi_5$	$3\times Ni_A$	Cu_5Ca	2.46	4	2.45	4	79, p. 1049
	$2\times Ni_B$		2.45	6	2.85	3	85, pp. 11,59
ThNi	Ni	FeB	2.69	2			91
Th_7Ni_3		Th_7Fe_3		0			80, p. 676, 85; pp. 17,135
UNi_5		Be_5Pd	2.40	6	2.83	12	85, pp. 13,107

La_7Pd_3, Ce_7Pd_3, and probably Al_3Pd where Table VIII shows no nearest-neighbor Pd-Pd contacts but the Pd *d*-band widths do vary widely. (V_3Pd=4.4 eV, La_7Pd_3=2.3 eV, Ce_7Pd_3=2.4 eV, and Al_3Pd =3.2 eV; see Tables IV and V.) Again this behavior cannot be explained in terms of Pd-Pd contacts.

When the above analysis is repeated for other Ni and Pd alloys with the help of Tables VII and VIII on crystal structures and Tables II—V on measured

TABLE VIII. Structures and Pd-Pd distances in Pd alloys. (N.B. The positions of atoms in unit cells with free coordinates are not always well defined; some of the interatomic distances given here were determined by analogy with more completely characterized compounds of a similar structural type.)

Compound	Structure type	r_1 Pd-Pd	CN	r_2 Pd-Pd	CN	References
Pd	A_1	2.75	12			82, pp. 121,148
$Al_{10}Pd_{90}$	Solution in Pd	2.75	11			79, p. 125; 83, p. 380
AlPd HT	FeSi	2.99	6			81, p. 35; 85, pp. 29,12
LT	Rhombohedral	2.92–3.02	6			81, p. 35; 85, pp. 15,12
Al_3Pd	Al_3Pd	?	?			80, p. 125; 84, pp. 6,705
ScPd	CsCl	3.28	6			81, p. 608
$TiPd_3$	Ni_3Ti	2.34?	4	2.74	4	82, p. 121; 85, pp. 38A,170
VPd	$TiAl_3$	2.72	4	2.73	4	80, p. 740; 85, pp. 26,165
VPd_2	$MoPt_2$	2.64	1	2.75	6	82, p. 121; 81, p. 614
VPd	Cubic	3.83				81, p. 614
V_3Pd	βW		0			80, p. 470; 83, p. 88
NiPd	Solid solution	2.64	6	Random dist.		83, p. 782
YPd_3	Cu_3Au	2.88	8			86, pp. 9,34
Y_7Pd_3	?	?	0?			
$LaPd_3$	Cu_3Au	3.00	8			86, pp. 9,34
$LaPd_2$	?	?	?			
LaPd	CrB	2.68	2			86, pp. 9,29
La_7Pd_3	Th_7Fe_3		0			86, p. 9
LaPdAl	Unknown	?	?	?	?	
$CePd_3$	Cu_3Au	2.93	8			86, pp. 9,34
Ce_3Pd_5	?	?	?	?	?	
CePd	CrB	2.66	2			86, pp. 9,29
Ce_7Pd_3	Th_7Fe_3		0			86, p. 9
CePdAl	Unknown					
$PrPd_3$	Cu_3Au	2.93	8			86, pp. 9,34
$NdPd_3$	Cu_3Au	2.92	8			86, pp. 9,34
$SmPd_3$	Cu_3Au	2.91	8			86, pp. 9,34
$TaPd_3$	$TiAl_2$	2.74	4	2.78	4	81, p. 609; 85, pp. 28,48
$TaPd_2$	$MoPt_2$	2.70	1	2.82 or 2.90	$4\times\frac{1}{2}$	81, p. 609; 85, pp. 30A,77
TaPd	TiCu	2.62	4			81, p. 609
$ThPd_3$	$TiNi_3$	2.63	4	2.92	4	80, p. 736; 84, Vol. 13, p.417
ThPd	FeB	2.78	2			81, p. 611; 83, p. 93
Th_2Pd	$CuAl_2$	2.97	4			81, p. 611
ThPdAl	Fe_2P		0			85, pp. 21,782
UPd_3	Ni_3Ti	2.88	4	2.93	4	82, p. 121; 85, pp. 19,249

d-band parameters, it becomes evident that a factor other than the Ni-Ni or Pd-Pd contacts is important in determining the *d*-band widths. We believe this factor is hybridization (mixing) between the levels of the Ni or Pd atoms and those of the neighboring atoms.

We find the description in terms of hopping integrals, as used in tight-binding calculations, most convenient to discuss the effects on bandwidths of hybridization (mixing) of states and the interaction between Ni or Pd atoms via the intermediate atoms. If we use *M*Ni as an example, we can say that the *d*-band width can arise from hopping of Ni electrons between the Ni atoms, or between the Ni atoms *via* the *M* atoms: these two effects are additive if not in a simple way. If the Ni-Ni distance is

increased and the number of Ni-Ni nearest neighbors is decreased then the Ni-Ni hopping integrals decrease, so that the Ni-*M*-Ni hopping becomes relatively more important. The Ni-*M*-Ni hopping integral is large if the overlap of Ni and *M* wave functions is large. Other things being equal, the hopping leads to large bandwidths if there are large numbers of states on the *M* site with energies similar to those on the Ni sites: For a given hopping integral the hybridization decreases with ΔE^{-1} where ΔE is the separation of the levels.

Using these ideas we may now rationalize the observations that for a given stoichiometry in Ni alloys, the order of Ni *d*-band widths is approximately Ni > Cr > Ta > Ti > Al > Sc > Mg > Th > Ce ~ La. (For Pd alloys the corresponding order of Pd *d*-band widths was Pd > Ta ~ V > Zr > Al > Th > Y ~ Ce ~ La.) There is a correlation between the DOS of the partner element (in eV^{-1}) in the region of the Ni or Pd *d* bands and the Ni or Pd *d*-band widths. Ce and La have narrow occupied bands only 1.5–2 eV wide so that in the Ce and La alloys the Ni and Pd bands are below the Ce and La bands. Th, Sc, and Ti are intermediate cases as the Ni and Pd bands overlap the bottom of the Th, Ti, and Sc bands. Mg and Al have wide *sp* bands whose DOS's at any one energy is not high (~0.3 electron states eV^{-1} $atom^{-1}$ in both cases) and the *d*-band widths are again intermediate in Ni-Pd or Mg-Al alloys. The *d* bands of V, Ta, and Cr have ~4–6 *d* electrons, and with widths of about 5 eV they have *about* 1 electron state eV^{-1} $atom^{-1}$ in the region of the Ni or Pd *d* bands. Alloys of V, Cr, and Ta with Ni or Pd have the largest Ni 3*d* or Pd 4*d* bandwidths of the alloys studied.

We believe that the results described in the preceding paragraph give convincing evidence that (a) Ni-*M*-Ni or Pd-*M*-Pd interactions give significant contributions to the Ni 3*d* or Pd 4*d* bandwidths, and (b) the contribution of Ni-*M*-Ni or Pd-*M*-Pd interactions to the bandwidths is larger when the second element, *M*, has a large DOS at the energy of the Ni or Pd *d* states. We imply here that when the element *M* has a large DOS at energy *E*, then so does the atom *M* in the alloy with Ni or Pd. This view is, in general, substantiated by the calculations.

We note also that the order of Ni or Pd *d*-band widths in alloys Cr ~ Ta ~ V > Zr ~ Ti > Al > Sc > Mg > Th > Y ~ Ce ~ La is very similar to the order of electronegativities.[103] Electronegativity is a complicated quantity whose interpretation in solid-state physics is not trivial. We thus suggest that our observations on bandwidths and state density may provide a more suitable starting point for the analysis of the interactions between the atoms of the alloys studied.

C. Bandwidth and structural stability

It is noteworthy that the 1:1 intermetallics have simple structures when the contribution of the neighboring atoms leads to large Ni or Pd *d*-band widths, as in the case of ScNi, TiNi, AlNi, or VPd. The 1:1 intermetallics in which the bands of the partner element only weakly overlap the Ni or Pd *d* bands have more complicated structures, often of boride or phosphide type. Further, the same elements whose 1:1 compounds have complicated structures also form intermetallic Ni or Pd compounds with complicated stoichiometrics and structures, e.g., the Th_7Fe_3-type compounds. The existence of such structures has in the past been correlated with electron-atom ratios and atomic-size ratios.[44–46,142,143] These correlations have proved useful, but we note that the Ni and Pd compounds listed in Tables VII and VIII are normally isostructural despite the approximately 10% difference in Ni and Pd atomic radii, and that structural types usually exist over large ranges of atomic-size ratios. The electron-atom ratios are, of course, the same in Ni and Pd compounds of the same stoichiometry, but they are also the same for TiNi and ThNi, which have different crystal structures.

Our results indicate a correlation between the existence of complicated structures and the lack of overlap in the energies of the Ni or Pd *d* bands with the *d* bands of the partner element. Note also that it is in similar situations that glassy-metal alloys can be prepared (see, e.g., Refs. 36–38).

The complicated structures of glassy-metal alloys and compounds like M_7Pd_3 or M_7Ni_3 bring some of the atoms into extremely close contact, and keep others further apart. We cannot yet say in what way this may be linked to bandwidths. Nevertheless we *speculate* that the lack of overlap of the bands in energy is a contributory *cause* of complicated structures in intermetallic compounds. We hope that this speculation may stimulate interest in the problem and help in design of experiments.

D. Ni and Pd *d*-band binding energies

The shifts of valence and core levels in XPS spectra on alloying are similar (see, e.g., Refs. 33 and

34). Table IX is a comparison of the shifts of the Ni $3d$ and Pd $4d$ (VB) centroids with the Ni $2p_{3/2}$ and Pd $3d_{5/2}$ core-level shifts from paper II. The degree of agreement is remarkable considering the experimental errors involved and suggests some physical implications.

Johansson and Mårtensson[144] have devised a simple Born-Haber scheme for interpreting the core-level shifts between atoms and solid elements. The scheme's principal assumption is that the valence-electron distribution on the core-ionized atoms is the same as that of an impurity atom with charge $Z+1$ in a matrix of metal atoms with charge Z. The scheme has been extended to alloys in Ref. 145 where the calculated shift of the A core levels in an alloy AB_x is given as

$$\Delta E_{\text{calc}} = E(A;AB_x) + E(A+1;A) - E(A+1;AB_x) + \cdots . \quad (1)$$

Here $E(A;AB_x)$ is the heat of solution of atom A in matrix AB_x; $A+1$ is the $Z+1$ element relative to A. The first term can be regarded as the change in the initial-state bonding properties while the second pair of terms represent the changes in the screened final state in the host A relative to that in the ma-

TABLE IX. Comparison of shifts in BE's of Ni and Pd core levels and VB centroids (in eV, + is a shift to higher BE).

Compound	Δ Ni $2p_{3/2}$	Δ VB	Compound	Δ Pd $3d_{5/2}$	Δ VB
$MgNi_2$	0.15	0	AlPd	1.85	1.8
Mg_2Ni	0.0	−0.05	Al_3Pd	2.5	2.5
$AlNi_3$	−0.05	0.1	ScPd	1.15	1.3
AlNi	0.1	0.25			
Al_3Ni_2	0.7	0.75	$TiPd_3$	0.6	0.5
Al_3Ni	1.05	1.1			
			VPd_3	0.4	0.5
ScNi	0.1	0.2	VPd_2	0.9	1.0
			VPd	0.9	1.3
TiNi	0.55	0.35	V_3Pd	1.3	1.6
$CrNi_2$	0.25	0.2	YPd_3	0.35	0.3
			Y_7Pd_3	1.55	1.5
InNi	−0.05	−0.35			
			$NbPd_2$	0.6	0.7
$TaNi_3$	0.05	0.0			
$TaNi_2$	0.5	0.6	$TaPd_3$	0.8	0.8
Ta_2Ni	0.6	0.7	$TaPd_2$	1.1	1.3
			TaPd	1.3	1.5
$LaNi_5$	−0.05	0.1			
$CeNi_5$	−0.1	−0.05	$LaPd_3$	0.55	0.2
$ThNi_5$	−0.1	0.0	$CePd_3$	0.6	0.8
			$PrPd_3$	0.35	0.5
$CeNi_2$	0.3	0.25	$NdPd_3$	0.5	0.5
			$SmPd_3$	0.6	0.5
LaNi	0.2[a]	0.25			
CeNi	0.3	0.3	$LaPd_2$	0.9	1.0
ThNi	0.3	0.45	Ce_3Pd_5	1.05	1.0
La_7Ni_3	0.05[a]	0.4	LaPd	1.2	1.2
Ce_7Ni_3	0.3	0.5	CePd	1.0	1.0
Th_7Ni_3	0.45	0.6	ThPd	1.4	1.6
			La_7Pd_3	1.35	1.2
			Ce_7Pd_3	1.4	1.4
La_3Ni	0.0[a]	0.4	Th_2Pd	1.5	1.7
			LaPdAl	1.4	1.5
			CePdAl	1.35	1.5
			ThPdAl	1.55	1.7

[a]Δ $2p_{1/2}$ binding energy.

trix AB_x.[144–146] A quantitative analysis of these terms was possible for dilute alloys in Ref. 145 and showed the first and third terms to be largest, and to partially cancel in many alloys. The middle term of Eq. (1) was always quite small ($\pm\sim 200$ meV).

The difference between the first and third terms of Eq. (1) is large if element A and $A+1$ have very different metallurgical properties. In nondilute alloys the third term cannot be evaluated accurately as it involves a ternary alloy,[146] but we can make a reasonable estimate if we consider it to be a weighted average of the energies $E(A+1;A)$ and $E(A+1;B)$. Let us consider the V-Pd alloys as an example. In the case of Pd, the $Z+1$ element is Ag. The alloying properties of Pd and Ag are very different.[79–82] Pd has quite a strong affinity for V, but Ag and V are immiscible, indicating an endothermic heat of solution of Ag in V and an endothermic contribution to $E(A+1;AB_x)$. However, the first term in Eq. (1), $E(\mathrm{V};\mathrm{VPd}_x)$, is significantly *exothermic,* so that the first and third terms do not cancel and large core-level shifts are observed.

The shifts of the valence levels also contain initial-state, or bonding, contributions. However, there are the additional effects of distortion of the bands due to correlation[12–15] and matrix-element effects.[100,101] The minimum statement that can be made on the basis of the similarity of core- and valence-level shifts in Table IX is that the differences in relaxation effects between core and valence electrons are nearly balanced by differences in initial-state, correlation, and matrix-element effects. Such a coincidental balance is unlikely unless the last three effects are small (say less than 200 meV). We thus believe the last three effects can be neglected here and that relaxation effects are quite similar for core electrons and the Ni $3d$ or Pd $4d$ valence electrons in Ni and Pd alloys. This may be at first sight surprising because the screening of the core holes in Ni is thought to be done largely by the $3d$ electrons.[144,147] In the Ni or Pd alloys where the d bands are often full, d electrons can still screen a core hole if the percentage of Ni or Pd d character on the core-ionized site is increased. For example if the d count on an Ni atom with "full" Ni d band is decreased from 10 to ~ 9 by hybridization in the initial state, then in the lowest-energy core hole, final-state screening effects increase the d count to nearly 10 (see paper II). The implication of the observation that screening or relaxation effects are similar for core and valence ionization in these alloys is that the final-state valence-band hole is (partially) localized, and similar to a core hole in its effects. The change in potential at the ionized site caused by this partially localized hole then increases the proportion of d character in the wave functions of the other electrons on the ionized site. A similar screening process has also been suggested to explain the O KLL Auger spectra from oxides.[148]

E. Comparison between theory and experiment

As mentioned throughout Sec. IV, the agreement between experiment and theory was not perfect. In general the calculated Ni or Pd d bands were narrower and their positions were not in good agreement with experiment. We now discuss whether the discrepancies can be attributed to known effects, such as those arising from the fact that in XPS one does not measure the eigenvalues calculated, or if other explanations must be sought.

The calculated widths include the contribution of the instrumental resolution, but not lifetime broadening due to decay of the hole in the VB holes created by photoemission. This decay leads to Lorentzian broadening of the spectrum, which is characterized by long tails. Such effects are certainly present in the experimental spectra, but there is also distinct broadening of the whole bands which often have a more rectangular shape than Lorentzian effects can explain. Good examples of these shapes are in Fig. 6 for InNi, ScNi, and TiNi. The comparisons made in these figures are between calculated one-electron DOS curves and energy distributions of excited states. These are not the same. Self-energy corrections to the XPS spectrum of Ni, for example, are known to remove intensity from the band into a satellite ~ 6 eV below E_F.[12–15] Because relatively more intensity is moved from the bottom of the band into the satellite, the XPS spectra underestimate the DOS at the bottom of the band and the intensity tails off. This *decreases* the experimental widths of the band. Such effects may also be present in Pd (Ref. 18) and VPd_3 or $TiPd_3$, but we usually observe the opposite effect, namely XPS peaks that are broader than the calculation. We can offer no satisfactory explanation for this effect.

A second problem arises with the measured and calculated d-band binding energies. Comparison of individual peaks is unreliable because of overlap of the peaks and the absence of multiple peaks in the XPS VB spectra due to the general broadening of the spectra. We thus compare the binding energies of the d-band centroids from XPS with the centroids of the calculated Ni and Pd d bands. In determining the centroids of the calculated d bands

we ignore the contribution of the "tails" to lower BE and the unoccupied Ni or Pd *d* character. The results are collected in Table X together with some results from the literature. The calculated *d* bands are, in general, deeper than found in experiment which contrasts with the results for Cu, Zn, Ga, etc. In those elements the *d*-level positions calculated are shallower than experiment and the discrepancy normally increases with increasing localization of the *d* levels. This is well known as a characteristic of local-density approximation.[75,76] In Ni itself this effect has been explained by correlation effects and the transfer of intensity from the bottom of the *d* bands to the 6-eV satellite. There is evidence against the general validity of this explanation for all the discrepancies found here. The "self-energy" explanation results in shifts of intensity into the satellite. If it were true here then the shifts should become systematically smaller in alloys with electropositive metals where the satellite is weaker. This is not the case. Although some isolated results, such as those for Al-Ni alloys, are in approximate agreement with this trend, others such as VPd and VPd_3 are not.

We suggest here a new line of investigation of this problem. Liebsch[15] showed figures of the spectral function due to a single-particle eigenvalue in Ni with a peak shifted to lower BE and a satellite to the high-BE side of the eigenvalue. This is another description of the effect of the nonlocal correction to the exchange-correlation term in the density-functional formalism. This correction, which is needed to calculate a true excitation spectrum, increases with the effective intra-atomic correlation energy, *U*. In general *U* is a function of the orbital and the atoms, so that the nonlocal correction to the eigenvalues needed to get an excitation spectrum is also a function of the orbital and the atom. Our suggestion is to use techniques like x-ray emission[99] or photoemission in Fano resonance (see, e.g., Refs. 149 and 150) to enhance the contribution to the different contributions from electrons in different states and compare these to the calculated DOS's of different states. If the disagreement is the same for the different states then its origin may not be these nonlocal corrections.[151]

We have made some preliminary attempt at this sort of experiment in this paper, for instance for Al-Pd alloys in Fig. 13. It is well known (see, e.g., Refs. 33, 34, 119, and 120) that a *d* band or resonance, such as Pd *d*, in an *s* band such as the Al *s* in AlPd, causes the *s*-state density to pile up and peak just below the *d* band. The energies of the two peaks (Al *s* and Pd *d*) are thus closely linked, before the nonlocal corrections are made. In AlPd and Al_3Pd the differences between theory and experiment were the same for the Al *s* states, studied by x-ray emission and the Pd *d* states studied by XPS. This suggests that nonlocal corrections do not cause the discrepancies and one may have to look for other effects. A full investigation should include variations of matrix elements and lifetime broadening through the bands, which are beyond the scope of this report. For this reason our conclusion remains tentative, but the differences deserve more attention. Note also that the observed shifts between theory and experiment are not so large that we must reject conclusions on the trends in hybridization, mixing, and charge transfer.

To summarize this section we may say that typi-

TABLE X. Comparison of calculated and experimental centroid positions (*C*) for the main (occupied) Ni and Pd *d* band peaks in Ni and Pd alloys (all values in eV).

	C				*C*		
Material	Expt.	Theor.	Expt.−Theor.	Material	Expt.	Theor.	Expt.−Theor.
Ni	1.4	1.9[a]	−0.5	AlPd	4.1	4.6	−0.5
$AlNi_3$	1.5	2.0	−0.5	Al_3Pd	4.8	4.1	0.7
AlNi	1.65	2.5	−0.85	ScPd	3.6	3.9	−0.3
Al_3Ni	2.5	2.6	−0.1	$TiPd_3$	2.8	3.4	−0.6
$Al_{97}Ni_3$	2.4[b]	1.8[c]	−0.6	Vpd_3	2.8	3.6	−0.8
ScNi	1.6	2.0	−0.4	VPd	3.3	4.4	−1.1
TiNi	1.75	2.8	−1.0	V_3Pd	3.6	4.2	−0.6
InNi	1.35	1.55	−0.2	YPd_3	2.6	2.6	0.0
NbNi	1.2[d]	2.5[d]	−1.3	Zr_3Pd	3.7[d]	3.9[d]	−0.2

[a]Reference 77.
[b]Reference 163.
[c]Reference 76.
[d]Reference 39. Experimental results here are from glassy alloys.

cal discrepancies between the *d*-band positions calculated and found experimentally by XPS are up to 1 eV in Ni and Pd alloys. It is unlikely that all the errors can be attributed to the fact that we calculate eigenvalues but measure ionization energies. We believe that one should consider more fundamental sources for the discrepancies. In this connection it should be noted that all computational methods have difficulty in calculating the energy required to transfer electrons between orbitals of different symmetries (see, e.g., Refs. 152 and 153). This is especially relevant in the alloys studied here, where the Fermi level is often in a region of largely *sp*-band character but peaks measured have largely *d*-band character.

F. *d*-band populations and a general model for Ni- and Pd-alloy electronic structure

In Sec. V C it was concluded that the Ni and Pd bands shift to higher BE's with respect to E_F in alloys with electropositive metals. In Sec. V B it was shown that the Ni and Pd *d* bands tend to narrow in alloys with electropositive elements. The combined effect is that the bands are being filled and the density of Ni or Pd states at E_F is dropping in such alloys. These observations explain the drop in electronic specific heats as well as the disappearance of magnetism in numerous such alloys, as discussed for specific cases in Sec. V.

In discussing our view of the *d*-band populations in Ni or Pd and their alloys we must constantly make the distinction between the number of electrons in the Ni or Pd *d* bands, and the number of Ni or Pd electrons on the Ni or Pd sites. For instance, Ni has 9.4 electrons in the *d* band.[61,62] The "*d*" states are hybrids, however, with a small amount of 4*s* character so that there are only approximately 8.8 Ni *d* electrons.[63] Alternatively we can say that the "*d* count" is 8.8.

We present our model of the electronic structure of alloys with electropositive metals schematically in Fig. 21. As a starting point we emphasize that the *s*, *p*, or *d* bands are in general not pure. The so-called Ni (or Pd) *d* bands which dominate the XPS spectra in most alloy studies, are mixed with some *s* character, which makes up about 10% of the total. Ni itself thus has 0.6 unoccupied states per atom in the Ni 3*d* band and there is some *d* character in other unoccupied bands. In all the Ni and Pd alloys the effective widths of the *d* bands decrease. This is especially noticeable in alloys with the electropositive metals. With introduction of electropositive metals the Ni or Pd *d* bands become filled, as shown in the lower part of Fig. 21. The Ni or Pd bands still contain some non-*d* character, as shown by our calculations. As described in Sec. II, we are unwilling to rely heavily on population analysis with the linear combination of atomic orbitals basis of our calculations for exact quantitative estimates of the amount of non-Ni *d* or non-Pd *d* character, primarily because of ambiguities arising from definition of the atomic boundaries. Nevertheless we do see from our calculations that the alloys retain some Ni or Pd *d* character in the unoccupied states, and that the total charge transfer to *d* orbitals at the Ni or Pd sites must be less than 0.4 electrons per site. The distribution of this unoccupied *d* character is very different from that in pure Ni. That its density at E_F is very low in alloys with electropositive metals is indicated by the experimental spectra, as well as by the calculations.

The changes in distribution of the occupied-*d*-state density have been extensively studied here by XPS. The changes in distribution of unoccupied states which are hypothesized on the basis of the XPS results and calculations will have several measurable characteristics which could be used to test the hypothesis.

(1) The valence- and core-level satellites in PS spectra will have different intensities. As shown in this paper, the decrease in VB satellite intensity in the alloys with electropositive metals is readily ob-

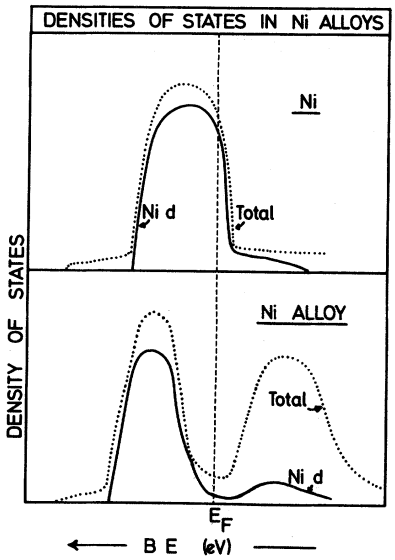

FIG. 21. Schematic model of the Ni *d*-state density in Ni and Ni alloys such as Sc-Ni. A similar model could be applied to Pd and Pd alloys. For further discussion see text.

servable, but not easily quantifiable because of overlap with the one-particle part of the VB. Paper II describes the decrease in satellite intensity in core levels.

(2) Spectroscopies of the unoccupied states, such as bremsstrahlung isochromat spectroscopy, should show changes in the distribution of unoccupied Ni or Pd d states. Isolated cases of such behavior are known[154] although they have not always been interpreted in terms of models like ours.

(3) Fano-resonance photoemission studies of the Ni valence states and satellites should show broader, weaker resonances. This is because the main channel in Fano resonance involves excitation from a core level to unoccupied Ni d states. In Ni itself most of the unoccupied d-state density is concentrated in a narrow region near E_F, leading to resonances whose width is largely determined by the core-level width. In the alloys studied here the unoccupied Ni d-state density is spread out, which should cause extra broadening of the resonance, and possibly weaken the resonance. It seems unrealistic to believe that the Ni d-state density could be spread out in states of predominantly "partner-element" character without changes in the values of the Fano line shapes.

(4) The Ni d character in Ni alloys with electropositive elements cannot lead to ferromagnetic behavior within the Stoner theory[155] because the DOS at the Fermi level is small. It is *possible* that such magnetism could result from the Ni d states in the newer covalent theory of magnetism[156] which only requires unoccupied-d character.

The diagram in Fig. 21 can be used to collate a very large amount of data besides the XPS spectra of Ni or Pd alloys with early transition metals. Similar trends are observed in spectra of Pt alloys[130,157] and also in some Co alloys.[158] The idea that the Ni or Pd band fills via admixture of character from the partner-atom wave functions explains equally well the observed changes in specific heat when electropositive metals are added to Ni or Pd (see, e.g., Refs. 61, 116, 124, and 125). It is also compatible with the drop in magnetic susceptibility in Pd and in the number of spins in Ni (Refs. 159–161) when small amounts of electropositive elements such as Al, Ti, or V are added to the pure metals.[162]

In the Ni or Pd alloys with sp metals studied here (Mg-Ni,Al-Ni,In-Ni,Al-Pd) or elsewhere [e.g., Mg-Pd (Ref. 24) or 2.8 % Ni in Al (Ref. 163)] the Ni or Pd d bands behave in much the same way as in alloys with early transition metals or rare earths. The Ni or Pd d bands become filled, are shifted from E_F, and are much narrower than in pure Ni. The only change in Fig. 21 required for the Ni or Pd sp metal alloys is a decrease in the total density of unoccupied states above E_F.

As the electronegativity difference between Ni and the partner element is decreased, the energy difference between the "effective atomic d levels"[164] decreases and it is necessary to introduce extra factors in order to explain the observations. In intermediate cases the Ni and partner-element bands *tend* to become less separated and more strongly mixed, as in Ni-Cr (Fig. 6) or Ni-Fe (Ref. 166) alloys and the alloys have a larger tendency to disorder.[79–85] Figure 22 illustrates the typical VB's of such alloys where the Ni and partner bands are so strongly mixed one can not speak of a separate Ni band that is pushed below E_F. This is seen in the XPS results as well as the specific-heat and magnetic susceptibility results of these alloys.[61,159–168]

We complete the scheme with noble-metal alloys. In Ni-Cu (Fig. 8, Refs. 104 and 105), Ni-Au (Fig. 8, Refs. 163 and 166), and Pd-Ag (Refs. 168 and 169) alloys, the effective atomic d levels have crossed so that the Ni or Pd bands lie in the sp bands above the noble-metal d bands. At low Ni or Pd concentrations in Au or Ag, respectively, the Ni or Pd d bands are narrow,[166,168,169] and there may be a low density of d states at E_F in Pd-Ag. At higher Ni or

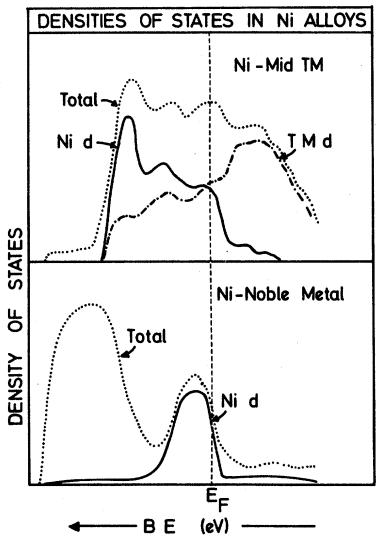

FIG. 22. Schematic diagram of Ni d-state and total state densities in alloys with elements of similar electronegativity, such as $CrNi_2$. A similar diagram could be applied to Pd or Pt alloys.

Pd concentrations the d bands broaden, principally because of Ni-Ni and Pd-Pd interaction, and the density of d states at E_F increases (see Fig. 8, Refs. 168 and 169). In Ni-Cu alloys this broadening causes the Ni and Cu d bands to overlap and leads to more effective mixing of the d levels.[105]

VI. CONCLUDING REMARKS

One of our hopes for this work is that it will help provide a basis for theoretical studies of alloy stability and structure. The heats of formation of binary intermetallic compounds may be as large as 1 eV, but this is still small compared to the total energy of the system. As the energy differences that stabilize a given structure type or lead to instability of a given phase with respect to disproportionation reactions are even smaller, an *ab initio* approach to their calculation is not always feasible. This leads to an interest in model calculations that only include the salient features of the VB structure. We believe that a sound and extensive basis of experimental data, as given here, is necessary to decide what are the salient features and help choose the most appropriate models.

For us one of the most satisfying aspects of this work was the emergence of trends in the electronic structure of Ni and Pd alloys with changing stoichiometry and partner element, and the correlation of such trends with known magnetic susceptibility and electronic specific-heat data. The advantage of XPS and calculations over the last two methods is that they give information on the whole occupied bands and not just a small portion at E_F. This makes it easier to detect and understand the trends in behavior.

In alloys with electropositive metals the Ni or Pd d bands are filled and moved away from E_F by increasing the concentration of the electropositive element. Mixing of the levels derived from the Ni or Pd and the electropositive metal is more important for this filling than charge transfer. As the electronegativity difference between the elements is decreased there is greater overlap in the band energies of the Ni or Pd and second metal so that it is more appropriate to speak of a common band. In such cases the relative weights of the Ni or Pd d character and second-metal character vary throughout the band. Furthermore, in these cases there is no sharp division between regions of Ni or Pd and second-metal character and no pronounced minima between two such regions. This explains why the characteristics of band filling, such as decreased electronic specific heat, are not observed in Ni or Pd alloys with late transition metals.

The widths of the Ni and Pd d bands decrease on dilution in electropositive metals, but the decrease is different for different metals. These decreases in width are never as strong as predicted on the basis of changes in direct Ni-Ni or Pd-Pd interactions. For a given stoichiometry, the measured widths of the Ni or Pd bands in alloys increase with the overlap in the energies of the bands of the pure metals. This effect is more important in alloys with other transition metals than in alloys with sp metals like Mg or Al.

We have found some significant differences between calculated DOS's and observed spectra. Not all of these are readily explained by the known effects of nonlocal corrections to the exchange-correlation term in the density-functional formalism. Further work is required to determine whether there is a new and fundamental effect causing these discrepancies.

ACKNOWLEDGMENTS

We thank Professor M. Campagna for his support and encouragement of this work. It is also a pleasure to acknowledge discussions with Y. Baer, P. H. Dederichs, W. Gudat, O. Gunnarsson, R. O. Jones, A. Liebsch, C. Monnier, and K. Schönhammer. The work could not have been completed without the technical assistance of M. Beyss, H. Gier, J. Keppels, U. Mambor, A. Schwarz, J.-M. Welter, and E. M. Wurtz.

APPENDIX: DERIVATION OF VB WIDTHS AND CENTROIDS

In this work the widths and centroids of the Ni and Pd d bands are of interest. In the photoelectron spectra these bands overlap with the emission from other bands. Interpretation is also complicated by the tail at high BE due to the d^8 satellite and the many-electron processes.[1–18,135,136] In addition the bands have broad tails due to lifetime broadening and instrumental broadening. In view of these effects all methods of extracting bandwidths and centroids have some limitation. Indeed it is more sensible for most purposes to define an "effective width" which cuts off the tails with, say, 5% of the intensity as this portion of the band determines most of the physical properties of the alloys. Here we give a synopsis of the methods used for fixing

the width and centroid positions.

The methods used to estimate the illustrated background are in Fig. 23. In the presence of a strong satellite we extrapolate a background from below the satellite, as in Fig. 23(d). In the absence of strong satellites a baseline tangential to the base on either side of the peak was drawn, as in Figs. 23(a)–23(c). In the case of alloys with elements such as La, the non-Ni or -Pd contribution to the observed spectra is concentrated near E_F. In such alloys we assumed the contribution from the non-Ni or -Pd to have the same width as in the pure element, and subtracted the contribution as shown in Fig. 23(c). In alloys of elements with broad bands, such as Al_3-Ni or Al_3-Pd, the Ni-Pd d levels sit on the broad ($\sim$10-eV) Al band, and we have extrapolated a background as in Fig. 23(a). The centroid was then calculated from the area left after background subtraction. In cases where the choice of background subtraction was ambiguous, choosing different methods made a difference of typically 0.2 eV.

In order to estimate the width of the Ni and Pd bands when they were clearly not cut by the Fermi level we extrapolated the line of greatest slope on either side of the peak down to the baseline. This procedure certainly overestimates the width by an uncertain amount. In the cases were the d bands cut the Fermi level we took the Fermi level as the top of the occupied band.

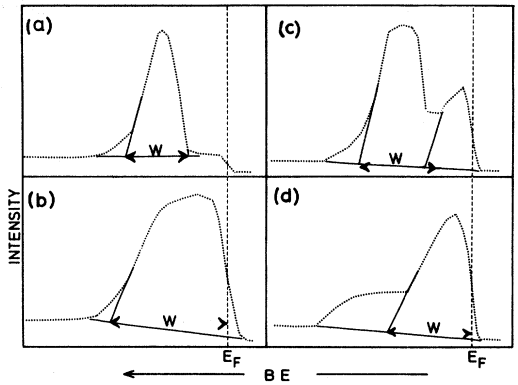

FIG. 23. Schematic diagram of the extraction of d-band widths in Ni and Pd alloys.

*Present address: Institute for Low Temperatures and Structure Research, Polish Academy of Sciences, 50-950 Wroclaw, Poland, POB 937.

†Present address: IE 350, Bell Telephone Labs., Murray Hill, New Jersey 07974.

[1]Y. Baer, P. F. Hedén, J. Hedman, M. Klasson, C. Nordling, and K. Siegbahn, Phys. Scr. 1, 55 (1970).

[2]S. Hüfner and G. K. Wertheim, Phys. Lett. 51A, 299 (1975); 51A, 301 (1975).

[3]P. C. Kemeny and N. J. Shevchik, Solid State Commun. 17, 255 (1975).

[4]C. Guillot, Y. Ballu, J. Paigné, J. Lecante, K. P. Jain, P. Thiry, P. Pinchaux, Y. Petroff, and L. Falicov, Phys. Rev. Lett. 39, 1632 (1977).

[5]R. J. Smith, J. Anderson, J. Hermanson, and G. J. Lapeyre, Solid State Commun. 21, 459 (1977).

[6]G. C. Tibbets and W. F. Egelhoff, Phys. Rev. Lett. 41, 188 (1978).

[7]M. Iwan, F. J. Himpsel, and D. E. Eastman, Phys. Rev. Lett. 43, 1829 (1979).

[8]J. Barth, G. Kalkoffen, and C. Kunz, Phys. Lett. 74A, 360 (1979).

[9]W. Eberhardt and E. W. Plummer, Phys. Rev. B 21, 3245 (1980).

[10]R. Clauberg, W. Gudat, E. Kisker, E. Kuhlmann, and G. M. Rothberg, Phys. Rev. Lett. 47, 1314 (1981).

[11]D. Penn, Phys. Rev. Lett. 40, 568 (1978); 42, 921 (1979).

[12]L. C. Davis and L. A. Feldkamp, J. Appl. Phys. 50, 1944 (1980); Solid State Commun. 34, 141 (1980); Phys. Rev. B 22, 3644 (1980).

[13]L. A. Feldkamp and L. C. Davis, Phys. Rev. Lett. 43, 151 (1980); 44, 673 (1980).

[14]A. Liebsch, Phys. Rev. Lett. 43, 1431 (1979).

[15]A. Liebsch, Phys. Rev. B 23, 5203 (1981).

[16]G. Treglia, F. Ducastelle, and D. Spanjaard, Phys. Rev. B 21, 3729 (1980).

[17]N. Mårtensson and B. Johansson, Phys. Rev. Lett. 45, 482 (1980).

[18]D. Chandesris, G. Krill, G. Maire, J. Lecante, and Y. Petroff, Solid State Commun. 37, 187 (1981).

[19]J. C. Fuggle, in *Electron Spectroscopy, Theory Techniques and Applications,* edited by C. R. Brundle and A. D. Baker (Academic, London, 1981), p. 85, and references therein.

[20]E. Antonides, E. C. Janse, and G. A. Sawatzky, Phys. Rev. B 15, 1669 (1977); 15, 4596 (1977).

[21]G. A. Sawatzky, Phys. Rev. Lett. 39, 504 (1977).

[22]M. Cini, Solid State Commun. 24, 681 (1977).

[23]M. Cini, Phys. Rev. B 17, 2788 (1978).

[24]P. Weightman and P. T. Andrews, J. Phys. C 13, 3529 (1980); 13, L815 (1980); 13, L821 (1980).

[25]G. Treglia, M. C. Desjonqueres, F. Daeastelle, and D. Spanjaard, J. Phys. C 14, 4347 (1981).

[26]T. Jach and C. J. Powell, Phys. Rev. Lett. 46, 953 (1981).

[27]J. C. Fuggle and Z. Zolnierek, Solid State Commun. 38, 799 (1981).
[28]F. U. Hillebrecht, J. C. Fuggle, P. Bennett, Z. Zolnierek, and Ch. Freiburg, following paper, Phys. Rev. B. 27, 2179 (1983).
[29]P. A. Bennett, J. C. Fuggle, F. U. Hillebrecht, A. Lenselink, and G. A. Sawatzky, this issue, Phys. Rev. B. 27, 2194 (1983).
[30]J. Hedman, M. Klasson, R. Nilson, C. Nordling, M. F. Sorokina, O. J. Kljushnikov, S. A. Nemnonov, V. A. Trapeznikov, and V. G. Zyryanov, Phys. Scr. 4, 193 (1972).
[31]S. Hüfner, G. K. Wertheim, and J. H. Wernick, Solid State Commun. 17, 1585 (1975).
[32]A. D. McLachlan, J. G. Jenkin, R. C. G. Leckey, and J. Liesegang, J. Phys. F 5, 2415 (1975).
[33]J. C. Fuggle, L. M. Watson, P. R. Norris, and P. J. Fabian, J. Phys. F 5, 590 (1975).
[34]J. C. Fuggle, E. Källne, L. M. Watson, and D. J. Fabian, Phys. Rev. B 16, 750 (1977).
[35]S. P. Kowalczyk, G. Apai, G. Kaindl, F. R. McFeely, L. Ley, and D. A. Shirley, Solid State Commun. 25, 847 (1978).
[36]P. Oelhafen, M. Liard, H.-J. Güntherodt, K. Berresheim, and H. D. Polaschegg, Solid State Commun. 30, 641 (1979).
[37]P. Oelhafen, E. Hauser, H.-J. Güntherodt, and K. H. Bennemann, Phys. Rev. Lett. 43, 1134 (1979).
[38]P. Oelhafen, E. Hauser, and H.-J. Güntherodt, in *Inner-Shell and X-ray Physics of Atoms and Solids,* edited by D. J. Fabian, H. Kleinpoppen, and L. M. Watson (Plenum, New York, 1981), p. 575.
[39]J. Kübler, K. H. Bennemann, R. Lapka, F. Rösel, P. Oelhafen, and H.-J. Güntherodt, Phys. Rev. B 23, 5176 (1981).
[40]P. Steiner, M. Schmidt, and S. Hüfner, Solid State Commun. 35, 493 (1980).
[41]P. T. Andrews, T. Collins, and P. Weightman, J. Phys. C 15, L3557 (1981).
[42]L. Pauling, *The Nature of the Chemical Bond,* 3rd ed. (Cornell University Press, Ithaca, 1960).
[43]L. Pauling, Proc. Natl. Acad. Sci. USA 36, 533 (1950).
[44]W. Hume-Rothery, *Elements of Structural Metallurgy* (Institute of Metals, London, 1961).
[45]*Charge Transfer/Electronic Structure of Alloys,* edited by R. E. Watson and L. H. Bennett (AIME, Warrendale, Penn., 1974).
[46]*Theory of Alloy Phase Formation,* edited by L. H. Bennett (AIME, Warrendale, Penn., 1980).
[47]A. R. Miedema and P. F. de Châtel, in *Theory of Alloy Phase Formation,* Ref. 46, p. 344.
[48]A. R. Miedema, F. R. de Boer, and R. Boom, J. Less-Common Met. 41, 283 (1975); 46, 67 (1976).
[49]A. R. Miedema, F. R. de Boer, and P. F. de Châtel, Physica B 100, 1 (1980).
[50]J. A. Alfonso and L. A. Girifalco, Phys. Rev. B 19, 3889 (1979).
[51]D. G. Pettifor, Phys. Rev. Lett. 42, 846 (1979).
[52]A. R. Williams, C. D. Gelatt, Jr., and V. L. Moruzzi, Phys. Rev. Lett. 44, 429 (1980); 44, 764(E) (1980).
[53]R. E. Watson, J. Hudis, and M. L. Perlman, Phys. Rev. B 4, 4139 (1971).
[54]T. S. Chou, M. L. Perlman, and R. E. Watson, Phys. Rev. B 14, 3248 (1976).
[55]T. K. Sham, M. L. Perlman, and R. E. Watson, Phys. Rev. B 19, 539 (1979).
[56]R. E. Watson and L. H. Bennett, Phys. Rev. B 15, 5136 (1977); 17, 3714 (1979); 18, 6439 (1978).
[57]R. E. Watson and L. H. Bennett, in *Theory of Alloy Phase Formation,* Ref. 46, p. 425.
[58]F. van der Woude and A. R. Miedema, Solid State Commun. 39, 1097 (1981).
[59]A. R. Williams, J. Kübler, and C. D. Gelatt, Jr., Phys. Rev. B 19, 6094 (1979).
[60]L. Hedin and B. I. Lundqvist, J. Phys. C 4, 2064 (1971).
[61]N. F. Mott, Adv. Phys. 13, 325 (1964).
[62]H. Danan, A. Herr, and A. J. P. Meyer, J. Appl. Phys. 39, 669 (1968), and references therein.
[63]See, e.g., L. Hodges, H. Ehrenreich, and N. D. Lang, Phys. Rev. 152, 505 (1966).
[64]D. Hackenbracht and J. Kübler, J. Phys. F 10, 427 (1980).
[65]A. Messiah, *Quantum Mechanics* (North-Holland, Amsterdam, 1961), Vol. I, p. 497.
[66]J. H. Scofield, J. Electron. Spectrosc. 8, 129 (1976).
[67]P. Hohenberg and W. Kohn, Phys. Rev. 136, B864 (1964).
[68]W. Kohn and L. J. Sham, Phys. Rev. 140, A1133 (1965).
[69]O. Gunnarsson and R. O. Jones, Phys. Scr. 21, 394 (1980).
[70]L. J. Sham and W. Kohn, Phys. Rev. 145, 561 (1966).
[71]A. R. Mackintosh and O. K. Andersen, in *Electrons at the Fermi Surface,* edited by M. Springford (Cambridge University Press, Cambridge, 1980).
[72]P. Thiry, D. Chandesris, G. Lecante, C. Guillot, R. Pinchaux, and Y. Petroff, Phys. Rev. Lett. 43, 82 (1979).
[73]V. L. Moruzzi, J. F. Janak, and A. R. Williams, *Calculated Electronic Properties of Metals* (Pergamon, Oxford, 1978).
[74]It is thought to be because of nonlocal corrections that the primitive potential of Chodorow [MIT Doctoral thesis, 1939 (unpublished)] gives somewhat better results for Cu [G. A. Burdick, Phys. Rev. 129, 138 (1963)] than the modern density-functional potentials in Ref. 73. See also Ref. 69.
[75]See, e.g., O. Gunnarsson, in *Electrons in Disordered Metals and Metal Surfaces,* edited by P. Phariseau *et al.* (Plenum, New York, 1981), p. 1.
[76]J. Deutz, P. H. Dederichs, and R. Zeller, J. Phys. F 11, 1787 (1981), and references therein.
[77]C. S. Wang and J. Callaway, Phys. Rev. B 15, 298 (1977); Physica 91B, 337 (1977); Phys. Rev. B 16, 2095 (1977).
[78]D. E. Eastman, F. J. Himpsel, and J. A. Knapp, J.

[79]M. Hansen and K. Anderko, *Constitution of Binary Alloys,* 2nd ed. (McGraw-Hill, New York, 1958).
[80]R. P. Elliot, *Constitution of Binary Alloys,* 1st Suppl. (McGraw-Hill, New York, 1965).
[81]F. A. Shunk, *Constitution of Binary Alloys,* 2nd Suppl. (McGraw-Hill, New York, 1969).
[82]C. J. Smithells, *Metals Reference Book,* 5th ed. (Butterworths, London, 1976).
[83]*Handbook of Lattice Spacings and Structures of Metals,* edited by W. Pearson (Pergamon, New York, 1958).
[84]*Powder Diffraction File* (JCPOS, International Center for Diffraction Data, Swarthmore, PA, 1979).
[85]*Metals and Inorganic Compounds,* in *Structure Reports,* edited by J. Trotter, C. A. Bear, J. M. Bree, and S. J. Rettig (Bohn, Scheltema, and Holkema, Utrecht, 1973), and references therein.
[86]A. Iandella and A. Palenzona, in *Handbook on Physics and Chemistry of Rare Earths,* edited by K. A. Gschneidner, Jr. and L. Eyring (North-Holland, Amsterdam, 1979), Vol. II, p. 1.
[87]P. I. Kripyakevich, E. I. Gladyshevskii, and E. N. Pylaeva, Kristallografiya 7, 212 (1962) [Sov. Phys.—Crystallogr. 7, 165 (1962)].
[88]*Constitution of Binary Alloys,* 2nd ed., Ref. 79, p. 888.
[89]C. J. Smithells, *Metals Reference Book,* 5th ed., Ref. 82, p. 698.
[90]P. Fischer, W. Hälg, L. Schlapbach, and K. Yvon, J. Less-Common Met. 60, 1 (1978).
[91]A. E. Dwight, M. H. Mueller, R. A. Conner Jr., J. W. Downwey, and H. Knott, Trans. Metall. Soc. AIME 242, 2075 (1968).
[92]J. C. Fuggle, H. Hanning, J. Keppels, and Z. Zolnierek (unpublished).
[93]C. Kittel, *Introduction to Solid State Physics,* 4th ed. (Wiley, New York, 1971), pp. 249ff.
[94]Note that we give the state density per atom rather than per unit cell because the number of atoms per unit cell is not constant.
[95]M. Dixon, F. E. Hoare, T. M. Holden, and D. E. Moody, Proc. R. Soc. London Ser. A 285, 561 (1965).
[96]W. de Dood and P. F. de Châtel, J. Phys. F 3, 1039 (1973).
[97]J. J. Begot, R. Caudron, P. Fairre, A. Lasalmonie, and P. Costa, J. Phys. (Paris) Lett. 35, L225 (1974).
[98]J. B. Dunlop, G. Grüner, and A. D. Caplin, J. Phys. F 4, 2203 (1974).
[99]D. J. Fabian, L. M. Watson, and C. A. W. Marshall, Rep. Prog. Phys. 34, 631 (1971), and references therein.
[100]A. Neckel, K. Schwarz, R. Eibler, P. Rastl, and P. Weinberger, Mikrochim. Acta, Suppl. 6, 257 (1975).
[101]D. W. Jennison, Phys. Rev. Lett. 40, 807 (1978).
[102]D. A. Papaconstantopoulos, J. W. McCaffrey, and D. J. Nagel, J. Phys. F 3, L26 (1973).
[103]W. Gordy and W. J. O. Thomas, J. Chem. Phys. 24, 439 (1955).
[104]S. Hüfner, G. K. Wertheim, R. L. Cohen, and J. H. Wernick, Phys. Rev. Lett. 28, 488 (1972).
[105]P. J. Durham, D. Ghaleb, B. L. Gyorffy, C. F. Hague, J. M. Mariot, G. M. Stocks, and W. M. Temmerman, J. Phys. F 9, 1719 (1979).
[106]*Handbook of Lattice Spacings and Structures of Metals,* Ref. 83, p. 782.
[107]J. Crangle and W. R. Scott, J. Appl. Phys. 36, 921 (1965), and references therein.
[108]G. Fischer, A. Herr, and A. S. P. Meyer, J. Appl. Phys. 39, 545 (1968).
[109]M. Hanson and K. Anderko, *Constitution of Binary Alloys,* 2nd ed., Ref. 79, p. 1048; R. P. Elliot, *Constitution of Binary Alloys,* 1st Suppl., Ref. 80, p. 676.
[110]S. Nasu, H. H. Neumann, H. Marzouk, R. S. Craig, and W. E. Wallace, J. Phys. Chem. Solids 32, 2779 (1971).
[111]T. Takeshita, K. A. Gschneidner, Jr., D. K. Thome, and O. D. McMasters, Phys. Rev. B 21, 5636 (1980).
[112]M. Cyrot and M. Lavagna, J. Phys. (Paris) 40, 763 (1979).
[113]J. Farrell and W. E. Wallace, Inorg. Chem. 5, 105 (1966).
[114]E. Burzo and J. Laforest, Int. J. Magn. 3, 171 (1972).
[115]D. Givord, F. Givord, D. Gignoux, W. C. Koehler, and R. M. Moon, J. Phys. Chem. Solids 37, 567 (1976).
[116]M. Glugla, H. G. Severin, and G. Sicking, Phys. Status Solidi B 106, 505 (1981).
[117]J. Wucher, Ann. Phys. Ser. 12 (France) 7, 317 (1952).
[118]J. J. Vuillemin and M. G. Priestley, Phys. Rev. Lett. 14, 307 (1965); Phys. Rev. 144, 396 (1966).
[119]F. Brouers, F. Cyrot-Lackman, and J. van der Rest, J. Phys. F 2, 1070 (1972).
[120]J. Kudrnovský, L. Smrčka, and B. Velický, in *X-ray Spectra and Electronic Structure of Matter,* edited by A. Faessler and G. Wiech (Fotodruck Frank OHG, München, 1973), Vol. II, p. 94.
[121]L. M. Watson, Q. S. Kapoor, and V. V. Nemoshkalenko, J. Phys. (Paris) 32, C4,325 (1971).
[122]F. L. Battye, H. Schulz, A. Goldmann, S. Hufner, D. Seipler, and B. Elschner, J. Phys. F 8, 709 (1978).
[123]The calculations were made for the ordered CsCl and Cu_3Au structures although the alloys show at least some disorder (Refs. 79 and 80).
[124]A. Obermann, W. Wanzl, M. Mahnig, and E. Wicke, J. Less-Common Met. 49, 75 (1976).
[125]G. Sicking, Z. Phys. Chem. (Wiesbaden) 116, 63 (1975).
[126]See R. P. Elliot, *Constitution of Binary Alloys,* 1st Suppl., Ref. 80, p. 265; F. A. Shunk, *Constitution of Binary Alloys,* 2nd Suppl., Ref. 81, p. 195.
[127]Shang-Lin Weng and M. El-Batanouny, Phys. Rev. Lett. 44, 612 (1980).
[128]M. El-Batanouny, M. Strongin, G. P. Williams, and J. Colbert, Phys. Rev. Lett. 45, 269 (1981).
[129]F. U. Hillebrecht and J. C. Fuggle, Phys. Rev. B 25, 3550 (1982).
[130]J. C. Fuggle and F. U. Hillebrecht (unpublished).
[131]K. Lang, Y. Baer, and P. A. Cox, J. Phys. F 11, 121 (1981).

[132]H. R. Ott, Y. Baer, and K. Andres, in *Proceedings of the International Conference on Mixed Valence Compounds, Santa Barbara, 1981,* edited by L. M. Falicov, W. Hanke, and M. B. Maple (North-Holland, Amsterdam, 1981), p. 297.

[133]Y. Baer, H. R. Ott, J. C. Fuggle, and L. E. De Long, Phys. Rev. B 24, 5384 (1981).

[134]Y. Baer, H. R. Ott, and K. Andres, Solid State Commun. 36, 387 (1980).

[135]S. Doniach and M. Sunjić, J. Phys. C 3, 285 (1970).

[136]H. Höchst, P. Steiner, and S. Hüfner, J. Phys. F 7, L309 (1977).

[137]J. C. Slater, *Quantum Theory of Atomic Structure* (McGraw-Hill, New York, 1960), Vol. II, p. 294.

[138]L. C. Davis (private communication).

[139]F. J. Himpsel and D. E. Eastman, Phys. Rev. B 18, 5236 (1978).

[140]O. K. Andersen, W. Klose, and H. Nohl, Phys. Rev. B 17, 1209 (1978).

[141]See also, J. W. Wilkins, Phys. Fenn. 8, 171 (1973).

[142]W. Hume-Rothery, in *Phase Stability in Metals and Alloys,* edited by P. S. Rudman, J. Stringer, and R. I. Jaffee (McGraw-Hill, New York, 1967), p. 3.

[143]K. A. Gschneidner, in *Theory of Alloy Phase Formation,* Ref. 46, p. 1.

[144]B. Johansson and N. Mårtensson, Phys. Rev. B 21, 4427 (1980).

[145]P. Steiner, S. Hüfner, N. Mårtensson, and B. Johansson, Solid State Commun. 37, 73 (1981).

[146]P. Steiner and S. Hüfner, Solid State Commun. 37, 79 (1981).

[147]L. Ley, S. P. Kowalczyk, F. R. McFeely, R. A. Pollak, and D. A. Shirley, Phys. Rev. B 8, 2392 (1973).

[148]J. C. Fuggle, E. Umbach, R. Kakoschke, and D. Menzel, J. Electron. Spectrosc. 26, 111 (1982).

[149]U. Fano, Comments At. Mol. Phys. 4, 119 (1973), and references therein.

[150]A. Kotani and Y. Toyozama, in *Synchrotron Radiation,* Vol. 10 of *Topics in Current Physics,* edited by C. Kunz (Springer, Berlin, 1979), pp. 196ff; K. Codling, *ibid.*, pp. 242ff, and references therein.

[151]The same arguments hold for the second sort of nonlocal correction, which leads to the eigenenergies of localized states being at higher BE than in experiment (see Refs. 67–76).

[152]J. Harris and R. O. Jones, J. Chem. Phys. 70, 830 (1979).

[153]O. Gunnarsson and R. O. Jones, J. Chem. Phys. 72, 5357 (1980); Solid State Commun. 37, 249 (1981).

[154]H. Föll, Z. Phys. B 26, 329 (1977).

[155]E. D. Stoner, Philos. Mag. 15, 1018 (1933); Proc. R. Soc. London Ser. A 154, 656 (1933); 165, 372 (1938); 169, 339 (1938); Rep. Prog. Phys. 11, 43 (1947).

[156]A. R. Williams, R. Zeller, V. L. Moruzzi, C. D. Gelatt Jr., and J. Kübler, J. Appl. Phys. 52, 2067 (1981).

[157]W.-D. Schneider and C. Laubschat, Phys. Rev. B 23, 997 (1981).

[158]A. Amanou, Solid State Commun. 33, 1029 (1980).

[159]D. Gerstenberg, Ann. Phys. (Leipzig) 2, 236 (1958).

[160]E. Kudiela-Artner and B. B. Argent, Proc. Phys. Soc. London 80, 1143 (1962).

[161]J. Crangle and G. C. Hallam, Proc. R. Soc. London Ser. A 272, 119 (1963).

[162]In writing up our ideas we recognized many similarities between the spirit of Fig. 21 and the ideas of Friedel expressed before the advent of photoemission (e.g., J. Friedel and A. Guinier, *Metallic Solid Solutions* (Benjamin, New York, 1963).

[163]P. Steiner, H. Höchst, W. Steffan, and S. Hüfner, Z. Phys. B 38, 191 (1980).

[164]The effective atomic level is the energy used as the starting energy in many calculations, see, e.g., Ref. 165.

[165]M. C. Desjonquères and M. Lavagna, J. Phys. F 9, 1733 (1979).

[166]A. Bosch, H. Veil, G. A. Sawatzky, and N. Mårtensson, Solid State Commun. 41, 355 (1982).

[167]K. Berndt, U. Marx, and O. Brümmer, Phys. Status Solidi B 90, 487 (1978), and references therein.

[168]A. D. McLachlan, J. Jenkin, R. C. G. Leckey, and J. Liesegang, J. Phys. F 5, 2415 (1975).

[169]G. M. Stocks, R. W. Williams, and J. S. Faulkner, J. Phys. F 3, 1688 (1973).